Available online at www.sciencedirect.com
ScienceDirect
Journal of Sound and Vibration 311 (2008) 1249–1270
JOURNAL OF SOUND AND VIBRATION
www.elsevier.com/locate/jsvi

# Effective properties of mechanical systems under high-frequency excitation at multiple frequencies

Jon Juel Thomsen*

*Department of Mechanical Engineering, Solid Mechanics, Technical University of Denmark, Building 404, DK-2800 Lyngby, Denmark*

Received 16 December 2006; received in revised form 3 October 2007; accepted 9 October 2007
Available online 26 November 2007

**Abstract**

Effects of strong high-frequency excitation at multiple frequencies (multi-HFE) are analyzed for a class of generally nonlinear systems. The effects are illustrated for a simple pendulum system with a vibrating support, and for a parametrically excited flexible beam. For the latter, theoretical predictions are supported by experimental observations, providing good agreement for a wide range of excitation conditions. The main effect of strong multi-HFE is to change the effective or apparent stiffness in a manner similar to that of mono-HFE, provided the HFE frequencies are well separated and non-resonant. Then the change in effective stiffness is proportional to the sum of squared excitation velocities, and the corresponding changes in equilibria, equilibrium stability, and natural frequencies can be computed as for the mono-HFE case. When there are two or more close-excitation frequencies, an additional contribution of slowly oscillating stiffness appears. This may cause strong parametric resonance at conditions that might not appear obvious, i.e. when the difference in two HFE frequencies is near twice an effective system natural frequency, which due to the HFE itself is shifted away from the natural frequency without HFE. Also, it is shown that strong multi-HFE can stabilize otherwise unstable equilibria, but generally this requires the frequencies to be well separated; thus, continuous broadband and random HFE does not have a uniquely stabilizing effect paralleling that of mono-HFE, or multi-HFE with non-close frequencies. The general results may be used to investigate or utilize general effects, or as a shortcut to calculate effective properties for specific systems, or to calculate averaged equations of motion that may be much faster to simulate numerically.


## 1. Introduction

The paper shows how effects of strong high-frequency excitation (HFE) having multiple frequencies (multi-HFE) can be conveniently analyzed, and concludes that most results for mono-HFE readily extend to the multi-HFE case. To illustrate basic principles, a simple example is first given (pendulum on a two-frequency oscillating support). Then a generalized nonlinear model is considered, which covers a broad range of applications. Finally, to illustrate an application of the general theory, a structural example (base-excited elastic string) is analyzed and tested experimentally. The theoretical results have been presented in a conference paper [1], along with preliminary experimental tests of qualitative features only. This present paper

*Tel.: +45 45 25 42 50; fax: +45 45 93 14 75.
*E-mail address:* jjt@mek.dtu.dk

0022-460X/$ - see front matter © 2007 Elsevier Ltd. All rights reserved.
doi:10.1016/j.jsv.2007.10.012

repeats the theoretical developments for completeness, and adds new experimental results providing good quantitative agreement for the effects of concern.

Strong HFE can change the effective properties of elastic structures in a manner that may not be obvious, or may be overlooked or misinterpreted when using pure numerical simulation or laboratory experiments. Even a zero-mean small-amplitude HFE may change structural features that may be essential for structural operation and safety, such as effective stiffness, natural frequencies, equilibria, equilibrium stability, and bifurcation paths, as has been known for many years [2–6]. Much has been learnt in recent years on such effects—for specific systems and for quite general classes of linear and nonlinear mathematical models—and well-proven methods exist for analyzing them (e.g., Refs. [7–13]). In most studies the HFE is assumed to be a stationary harmonic mono-frequency function of time. However, in applications multi-HFE is not uncommon—either with a few frequencies (e.g., structures connected to multiple imbalanced rotors), with many discrete frequencies (e.g., higher harmonics of non-harmonic time-functions), or with a continuous spectrum of high frequencies (HFs) (e.g., structures connected to rocket or jet engines).

There are many studies of various effects of multi-frequency excitation, of which in particular the possibility of combination resonances for nonlinear systems is important, and thoroughly treated by Nayfeh and coworkers in e.g. Refs. [14,15]. Also, Nayfeh and Nayfeh [16] analyzes the response of a single-degree-of-freedom system with cubic nonlinearity to slowly modulated HFE, effectively corresponding to a three-frequency excitation with close frequencies. In these studies the multi-frequency excitation is not supposed to be strong and of high frequency, and thus effects such as apparent stiffening, of concern in the present study, do not show up.

There seems to be rather few studies dealing with effects of strong multi-HFE: Chelomei [17] considered the effect of multi-HFE for a general class of systems, focusing on its effect on the stability of equilibria of linear systems. Bogdanoff and Citron [18] studied linear systems with multi-HFE, and showed that a pendulum on a vibrating support can be stabilized in the inverted position by random multi-HFE, provided the frequencies of the HFE are not close. Hemp and Sethna [19] contributed a thorough, mathematically oriented investigation of general nonlinear dynamical systems in the Hamiltonian form, with particular focus on effects of simultaneous fast and slow parametric excitation. Kovaleva [20] examined the stability of discrete dynamical systems in a general Hamiltonian form and showed, generally and by physical examples, that multi-HFE having random and quasi-periodic components can be used to generate new, stable equilibria. These studies [17–20] do not include consideration to the influence of resonance, which is important for the analysis of continuous elastic structures.

The analysis of continuous elastic structures with HFE introduces special problems. This is because asymptotic analysis of HF-excited systems usually assumes the excitation frequencies are far beyond the linear natural frequencies of the system, leading to approximate expressions for the fast components of motion that ignores any influence of possible resonances. With HF-excited continuous elastic structures, as e.g. the beams, columns, and spinning discs investigated in Refs. [21–26], this assumption is questionable, since the modal density is typically so high that resonances are affecting the response in most of the relevant frequency range. Thus care must be taken to restrict the frequency range of application to non-resonant regimes, or the influence of resonance must explicitly be taken into account, as in Ref. [26] for a beam system. This present work incorporates the general consideration of resonant influence (but not exact or *sharp* resonance), in a manner that adds only marginally to computational burden and complexity.

The general class of systems covered by this work extends [12] in two respects: first the type of HFE under consideration is extended from mono-frequency with a short period, to generally multi-frequency with any period (including infinite, corresponding to quasi-periodic HFE). Secondly, consideration of weakly resonant effects is directly incorporated, which means that the multi-HFE frequencies do not need to be much larger than the linear resonances of the system. This makes the results directly applicable also to discretized models of continuous elastic systems.

Next we present an example to illustrate, in a simple setting, various effects that can occur with multi-HFE. Then a very general class of systems is considered, and correspondingly general results are derived using the method of direct separation of motions [7]. Finally, the general results are employed to predict how the apparent stiffness of an elastic string changes in response to multi-HFE, and the predictions are tested against laboratory experiments.

## 2. Example I: Illustrating the main effects of multi-HFE

Consider a pendulum in gravity $g$ (Fig. 1), whose support vibrates vertically and harmonically in time $\tilde{t}$, at multiple frequencies $\tilde{\Omega}_j$ being much higher than the natural frequency $\omega_0 = \sqrt{g/l}$, with corresponding amplitudes $A_j l$ much smaller than the pendulum length $l$. The pendulum swing $\theta(t)$ is governed by the non-dimensional equation of motion:

$$\ddot{\theta} + 2\beta\dot{\theta} + (1 + \ddot{q}(t)) \sin\,\theta = 0, \qquad q(t) = \sum_{j=1}^{m} A_j \sin(\Omega_j t + \alpha_j),$$
$$A_j \ll 1, \quad \Omega_j \gg 1, \quad \Omega_j A_j = O(1), \quad \beta \ll 1, \tag{1}$$

where time and frequencies have been normalized by $\omega_0$, i.e., $t = \omega_0 \tilde{t}$ and $\Omega_j = \tilde{\Omega}_j/\omega_0$, and overdots denote derivatives with respect to $t$. The definition of $q$ and the last two assumptions in Eq. (1) implies that $\ddot{q} = O(\Omega_j^2 A_j) = O(\Omega_j) \gg 1$, and thus the excitation term is assumed to be "stronger" than the stiffness term.

The system (1) belongs to a general class of discrete dynamical systems to be analyzed in Section 3. This present section aims at illustrating the effects of concern in a simple physical setting, so here we bypass all intermediate calculations and simply present the final outcome of applying the general results of Section 3: The pendulum motions $\theta$ are approximately—to order $\Omega^{-1}$, where $\Omega = m^{-1}\sum_{j=1}^{m}\Omega_j$ is the average high excitation frequency—given by

$$\theta(t) = z(t) + \Omega^{-1}\varphi(t, \Omega t), \quad \Omega^{-1} \ll 1, \tag{2}$$

where $z$ and $\varphi$ are of magnitude order unity. Here the first term $z(t)$ holds the slow or average component of $\theta$, which is governed by

$$\ddot{z} + 2\beta\dot{z} + \left(1 + \Omega^2 \sum_{i,j=1}^{m} \sigma_{ij}^2(t) A_i A_j \cos\, z\right) \sin\, z = 0, \tag{3}$$

with $\delta_{ij}$ denoting Kronecker's delta:

$$\sigma_{ij}^2(t) = \begin{cases} \dfrac{\Omega_i \Omega_j}{2\Omega^2}\delta_{ij} & \text{for} \quad |\Omega_i - \Omega_j| \gg 1, \quad i,j = 1,\ldots,m, \\ \frac{1}{2}\cos((\Omega_i - \Omega_j)t + \alpha_i - \alpha_j) & \text{for} \quad |\Omega_i - \Omega_j| \leqslant O(1), \end{cases} \tag{4}$$

and the initial conditions $z(0)$ and $\dot{z}(0)$ are determined by

$$z(0) - \sin\, z(0) \sum_{j=1}^{m} A_j \sin(\alpha_j) = \theta(0), \quad \dot{z}(0) = \dot{\theta}_0 + \sin\, z(0) \sum_{j=1}^{m} A_j \Omega_j \cos(\alpha_j). \tag{5}$$

The second term $\Omega^{-1}\varphi$ in Eq. (2) is a small overlay of HF-oscillations:

$$\Omega^{-1}\varphi(t,\tau) = -\sin\, z \sum_{j=1}^{m} A_j \sin(\Omega_j t + \alpha_j) + O(\Omega^{-2}). \tag{6}$$

The splitting in Eq. (2) of motions into slow components $z$ and small but fast components $\varphi$ would follow as a result of using, e.g., averaging or multiple scales perturbation analysis, or it can be considered an assumption to be checked *a posteriori*. The relevance of this assumption can be understood physically, by considering how

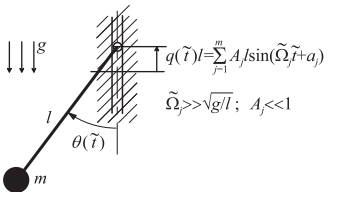


Fig. 1. Pendulum with a support that vibrates at multiple high frequencies.

HF inputs are filtered through the specific system: The unexcited part of Eq. (1) has the function of low-pass filtering the displacement input (here $q(t)$), so that any displacement input at a frequency substantially higher than the linear natural frequency (here $O(1)$) will only produce a small or even vanishing displacement output at that frequency. The only way a small-amplitude HF input in Eq. (1) can produce a large HF output would be by resonance, which is precluded here by the assumption $\Omega \gg 1$. The fast components of velocity and acceleration (and thus force) are not small, however; as Eq. (2) implies directly, they are $O(1)$ and $O(\Omega) \gg 1$, respectively.

Of primary interest here is Eq. (3), for the slow pendulum motions $z$, while the fast but small motions $\Omega^{-1}\varphi$ are usually interesting only by their effect on $z$. The main effects of multi-HFE depend on whether two or more of the excitation frequencies $\Omega_j$ are close, or if they are all well-separated; we next consider each of these cases.

### 2.1. Case: Multi-HFE with non-close frequencies

When all the excitation frequencies $\Omega_j$ are high and well-separated, $|\Omega_i - \Omega_j| \gg 1$, the functions ${\sigma_{ij}}^2$ are given by the upper expression in Eq. (4), which inserted into Eq. (3) gives

$$\ddot{z} + 2\beta\dot{z} + (1 + v^2 \cos z)\sin z = 0, \tag{7}$$

where the constant $v^2$ expresses the intensity of the HFE, which is proportional to the sum of squared excitation velocities:

$$v^2 = \frac{1}{2}\sum_{j=1}^{m}(\Omega_j A_j)^2. \tag{8}$$

Eq. (7), governing the slow component $z$ of $\theta$, is similar to Eq. (1) for the full pendulum motions $\theta$, though with the non-autonomous excitation terms replaced by an averaged effect of these. Also, Eq. (7) is identical to the averaged equation for the case of mono-HFE [11,13], where $m = 1$ and $v^2 = (\Omega A)^2/2$. Thus the presence of multiple non-close frequencies is accounted for solely by the definition (8) of the excitation intensity.

As appears when letting $\ddot{z} = \dot{z} = 0$ in Eq. (7), there are at least two equilibria for the slow pendulum motions: $z = 0$ and $z = \pi$, corresponding to $\theta = 0$ (down-pointing pendulum) and $\theta = \pi$ (up-pointing pendulum). To study motions near these, we linearize Eq. (7) near each

$$\ddot{z} + 2\beta\dot{z} + \omega_0^2 z = 0, \quad \text{for } z \approx 0, \tag{9}$$

$$\ddot{z} + 2\beta\dot{z} + \omega_\pi^2 (z - \pi) = 0, \quad \text{for } z \approx \pi, \tag{10}$$

where the linear stiffness coefficients are

$$\omega_0^2 = v^2 + 1, \quad \omega_\pi^2 = v^2 - 1. \tag{11}$$

The linear stiffness coefficient $\omega_0^2$ for Eq. (9) increases with the HFE intensity $v^2$, and is always positive; hence, the equilibrium $z = 0$ is always stable to small disturbances. Also, as $v$ is increased, the (non-dimensional) frequency $\omega_0$ of small oscillations near $z = 0$ increases from unity to $\sqrt{1 + v^2}$, so that the pendulum oscillates faster about its down-pointing equilibrium in the presence of HFE.

In Eq. (10) the linear stiffness coefficient $\omega_\pi^2$ also increases with the HFE intensity $v^2$. When $v^2 < 1$ the stiffness coefficient is negative, so that the up-pointing equilibrium is unstable, whereas if $v^2 > 1$ the stiffness is positive and the pendulum is stable in the up-pointing position (as reported in numerous studies since [2,3]). In the latter case small oscillations near $z = \pi$ occur at frequency $\omega_\pi = \sqrt{v^2 - 1}$, which increases from zero as the HFE intensity is increased beyond the critical value $v^2 = 1$.

In addition to the equilibria at $z = 0$ and $z = \pi$, when $v^2 > 1$ two new equilibria emerge at $z = \pm \arccos(-v^{-2})$, symmetrically about the vertical axis of gravity, and moving smoothly from $z = \pi$ towards $\pi \pm \pi/2$ as $v^2$ is increased from 1 to infinity. These equilibria are always unstable, and act as potential barriers between the equilibria at $z = 0$ and $z = \pi$, which are both stable when $v^2 > 1$.

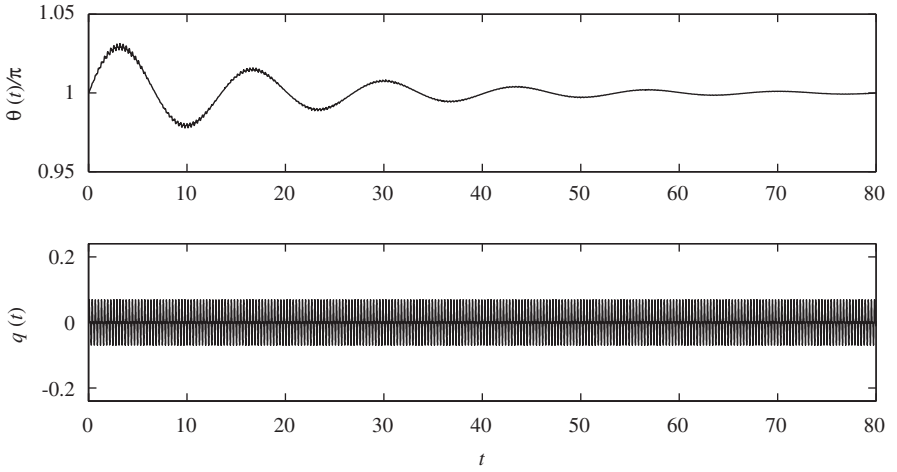


Fig. 2. Damped pendulum oscillations $\theta(t)$ (upper time series) towards the inverted position $\theta = \pi$, which is stabilized by small-amplitude support motions $q(t)$ (lower time series) at two non-close, high frequencies, as obtained by numerical simulation of the equation of motion (1). Parameters: $\beta = 0.05$, $\Omega_1 = 20$, $\Omega_2 = 40$, $A_1 = 0.05$, $A_2 = 0.03$, $\alpha_1 = \alpha_2 = 0$, $\theta(0) = \pi$, $\dot{\theta}(0) = 0.05$.

Thus, the HFE causes several changes in the effective properties of the pendulum system: new equilibria are created, the effective natural frequencies are changed, and the stability of existing equilibria is changed. All these effects are typical for HF-excited systems, and originate from a change in effective stiffness.

To illustrate a quantitative application of the above results, Fig. 2 shows a time series obtained by numerical simulation (using the MATLAB-function ode45) of the original system (1) with two-frequency HFE, with parameters as given in the figure legend. The pendulum is initially positioned at $\theta = \pi$, and at $t = 0$ given a small velocity disturbance $\dot{\theta}(0)$. The simulated time series shows damped slow oscillations towards the inverted equilibrium $\theta = \pi$, with an average period of $T = 13.39$, and a small HF-overlay of the magnitude order of the HFE amplitudes. With the present parameters Eq. (8) gives $v^2 = 1.22 > 1$, so that the equilibrium $z = \pi$ should be stable to small disturbances (while if only one of the two excitations were applied then $v^2 < 1$, and $z = \pi$ would be unstable). Furthermore, small oscillations about the stable equilibrium should occur at angular frequency $\omega_\pi = \sqrt{v^2 - 1} = 0.4690$, corresponding to a period of $T = 2\pi/0.4690 = 13.40$ thus agreeing rather accurately with the simulation result $T = 13.39$. The agreement will decrease as the assumption ceases to be fulfilled, i.e. as the excitation frequencies become lower and closer, and the HFE amplitude becomes larger.

It appears that for non-close high frequencies the slow effects of multi-HFE do not differ from the case of mono-frequency excitation, if just the excitation intensity is calculated as a sum of squares of the intensities at each frequency, *cf.* Eq. (8).

### 2.2. Case: Multi-HFE with close frequencies

When two or more of the high excitation frequencies are close, i.e. $O(1)$ or smaller, the functions ${\sigma_{ij}}^2$ are given by the lower expression in Eq. (4), which inserted into Eq. (3) gives

$$\ddot{z} + 2\beta\dot{z} + (1 + (v^2 + p(t)\cos z)\sin z = 0, \tag{12}$$

where $v^2$ is still given by Eq. (8), while

$$p(t) = \sum_{i=1}^{m-1} \sum_{j=i+1}^{m} \Omega^2 A_i A_j \cos((\Omega_i - \Omega_j)t + \alpha_i - \alpha_j). \tag{13}$$

Comparing to the similar expression (7) for the case of non-close excitation frequencies, we see that the averaged effect of the presence of close frequencies corresponds to a parametric excitation, oscillating at the small difference frequencies $\Omega_i - \Omega_j$.

The interaction between the change in effective stiffness (the $v^2$-term) and parametric excitation may create slow effects that may not be obvious when considering only Eq. (1) for the full motions: As is well-known [14], primary parametric resonance may occur when a parametric excitation frequency is near twice the linear natural frequency of a system. For the present system this means any $|\Omega_i - \Omega_j|$ coming near twice the *effective* natural frequency, and this natural frequency may be shifted away (by the $v^2$-term) from the corresponding natural frequency of the unexcited pendulum.

To study motions near the static equilibria $z = 0$ and $z = \pi$ we linearize (12) near each of them and obtain

$$\ddot{z} + 2\beta\dot{z} + (\omega_0^2 + p(t))z = 0 \quad \text{for } z \approx 0, \tag{14}$$

$$\ddot{z} + 2\beta\dot{z} + (\omega_\pi^2 + p(t))(z - \pi) = 0 \quad \text{for } z \approx \pi, \tag{15}$$

where the linear stiffness coefficients $\omega_0^2$ and $\omega_\pi^2$ are still given by Eq. (11).

With Eq. (14) being a damped Hill-equation, the down-pointing equilibrium $z = 0$ of the pendulum may be destabilized by parametric resonance when $|\Omega_i - \Omega_j| \approx 2\omega/k$, $k = 1, 2, \ldots$, and the corresponding excitation amplitude $\Omega^2 A_i A_j$ is beyond a critical value. The nearness to resonance and critical amplitude for this to occur can be calculated using standard results for the Hill-equation as given in many texts (e.g., Ref. [14]), as can the resulting nonlinear response under resonant conditions (in Ref. [11] this is done for a system similar to Eq. (12)). Though, when using results from perturbation analysis, care should be taken to check the accuracy, since the excitation amplitudes $\Omega^2 A_i A_j$ are $O(1)$ , and thus not small compared to the stiffness coefficient $\omega_0^2$.

To illustrate the effect of parametric resonance at a shifted frequency, Fig. 3 shows a time series obtained by numerical simulation of the original system (1) with two-frequency HFE, with parameters as given in the figure legend, and initially transients discarded. The resulting stationary oscillations of the pendulum (upper time series) have a slow period $T = 4.833$, and is resonant in character with a large-amplitude ($O(1)$) compared to the small-amplitude ($O(\Omega^{-1})$) input. Considering Eq. (14) and the remarks below, this could be expected, since with the present parameters the frequency difference $|\Omega_1 - \Omega_2| = 2.6$ is close to twice the effective natural frequency $2\omega_0 = \sqrt{v^2 + 1} = 2\sqrt{1 + \frac{1}{2}(\Omega_1 A_1)^2 + \frac{1}{2}(\Omega_2 A_2)^2} = 2.831$. The pendulum should then perform parametrically resonant oscillations at half the difference in excitation frequencies, i.e. $(\Omega_2 - \Omega_1)/2 = 1.3$, corresponding to a period of $T = 2\pi/1.3 = 4.833$, which agrees with the simulated time series. Considering just the original equation of motion (1), one might not think that large responses could occur under the above conditions, while this appears more readily from the averaged system (12).

As for the up-pointing equilibrium $z = \pi$ of Eq. (15), it cannot—as for the case of non-close frequencies—be stabilized simply by ensuring $\omega_\pi^2 > 0$, since parametric resonances at $|\Omega_i - \Omega_j| \approx 2\omega_\pi/k$, $k = 1, 2, \ldots$ may

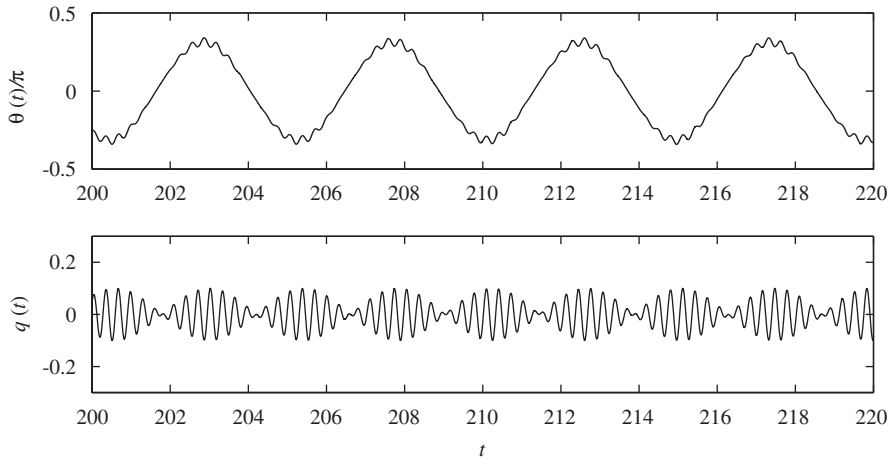


Fig. 3. Large stationary pendulum motions $\theta(t)$ (upper time series) induced by small-amplitude support motions $q(t)$ (lower time series) at two close high frequencies, as obtained by numerical simulation of the equation of motion (1). Parameters: $\beta = 0.05$, $\Omega_1 = 18.7$, $\Omega_2 = 21.3$, $A_1 = A_2 = 0.05$, $\alpha_1 = \alpha_2 = 0$, $\theta(0) = 0.01$, $\dot{\theta}(0) = 0$.

destabilize $z=\pi$ when an HFE amplitude $\Omega^2 A_i A_j$ exceeds a critical value. With increased values of $\Omega^2 A_i A_j$, the width of the resonant regions increase (cf. the classical Strutt diagram [14]), so that $z=\pi$ is stable for narrower ranges of parameter values. Similarly, for the case $\omega_\pi^2<0$ (where $z=\pi$ is always unstable with *non*-close HFE), a narrow range of parameter values rendering $z=\pi$ stable do exist (cf. the only stable region in the fourth quadrant of the Strutt diagram: a narrow "tongue"), but for typical parameter values of the assumed magnitude order the equilibrium $z=\pi$ is unstable.

Hence, stabilization of the inverted pendulum position requires either strong mono-HFE or strong multi-HFE with frequency separations being larger in magnitude order than the unforced natural frequency, or—if there are close excitation frequencies—some special combination of parameter values. With continuous broadband or random HFE, the requirement of frequency separation cannot be fulfilled: there will always be parametrically resonant (and thus destabilizing) frequency differences, at least for small damping. These conclusions agree with Refs. [18,19].

Observations similar to some of those above were derived and reported by Fidlin in Section 6.3 of Ref. [10], on illustrating the effect of a slowly modulated parametric HFE for a pendulum; Note here that a slowly modulated HF signal is equivalent to a pair of HF signals being close in frequency, e.g., $\sin((\Omega+\Delta\Omega)t)+\sin((\Omega-\Delta\Omega)t)=2\cos(\Delta\Omega t)\sin(\Omega t)$, where $2\Delta\Omega\ll\Omega$ is the frequency spacing, and $\Delta\Omega$ the modulation frequency.

## 3. Results for a general class of systems

With the above specific example in mind to ease interpretation, we next consider a quite general class of discrete dynamical systems with multi-HFE, covering a broad variety of applications. The purpose of the analysis is to determine the slow or averaged components of motions, which will be those apparent to lowpass-filtering observers such as measuring instruments and human senses. The analysis can be performed using different perturbation techniques, considering $\Omega^{-1}$ as a small parameter where $\Omega$ is a characteristic large excitation frequency. Standard averaging can be used as in Ref. [10], or multiple time scaling methods as in Refs. [22,24,27], or the method of direct separation of motions (MDSM) as in a large number of studies (e.g., see Refs. [7–13,28] and references cited there). In Refs. [10,13] these techniques are briefly compared, and shown to give identical or similar results, though with the MDSM being computationally more convenient.

### 3.1. The general system

Consider discrete mechanical systems modeled by

$$\mathbf{M}(\mathbf{u},t)\ddot{\mathbf{u}}+\Omega^2\mathbf{K}\mathbf{u}+\mathbf{s}(\mathbf{u},\dot{\mathbf{u}},t)+\sum_{j=1}^{m}(\mathbf{h}_j(\mathbf{u},\dot{\mathbf{u}},t)+\Omega\mathbf{f}_j(\mathbf{u},t))\frac{\partial^2\xi_j(t,\tau)}{\partial\tau^2}=\mathbf{0},$$
$$\mathbf{u}=\mathbf{u}(t),\quad \mathbf{u}(0)=\mathbf{u}_0,\quad \dot{\mathbf{u}}_0(0)=\dot{\mathbf{u}}_0,\quad \tau=\Omega t,\quad \Omega\gg 1, \tag{16}$$

which covers numerous applications, see e.g. Refs. [11,13]. It is an extension of the one analyzed in Ref. [12], and compared to the (in other respects more general) system considered in Section 4.3 of Ref. [7] it holds a term $\Omega^2\mathbf{K}\mathbf{u}$ that allows analysis of resonant influence. Here $\mathbf{u}(t)\in D\subset R^n$ describes positional state with corresponding velocities $\dot{\mathbf{u}}=\mathrm{d}\mathbf{u}/\mathrm{d}t$, $\mathbf{M}$ is a positive definite mass matrix, $\Omega^2\mathbf{K}$ is a constant matrix describing linear stiffness or restoring force, $\mathbf{s}$ holds the 'slow' forces, and $\mathbf{h}_j$, $\mathbf{f}_j$, and $\xi_j$ jointly describe the multi-HFE of characteristic frequency $\Omega\gg 1$, i.e. the 'fast' forces. The sum of fast forces, along with its first and second derivative with respect to $\tau$, is supposed to have zero fast-time average (any non-zero average being included in $\mathbf{s}$ or $\mathbf{K}\mathbf{u}$), and to be $T$-periodic and square-integrable in $\tau$, where $T\in]T^*;\infty[$, $T^*=O(2\pi/\Omega)$, with the fast-time average of a function $\mathbf{g}(t,\tau)$ defined by

$$\langle\mathbf{g}(t,\tau)\rangle_\tau\equiv\frac{1}{T}\int_0^T\mathbf{g}(t,\tau)\,\mathrm{d}\tau, \tag{17}$$

where the integration is performed with the slow time $t$ considered fixed. All functions in Eq. (16) are generally nonlinear and of magnitude order unity $O(1)$ or lower, $\xi_j$ are bounded on $[0;T]$, and $\mathbf{f}_j$ and $\mathbf{M}$ are bounded on

the subset $D$ with continuous first derivatives with respect to $\mathbf{u}$ (whereas $\mathbf{h}_j$ and $\mathbf{s}$ need not to be continuous). Terms multiplied by the large parameter $\Omega$ are considered 'strong'.

We note for illustration that the equation of motion (1) for the pendulum in multi-HFE belongs to the class (16), with $n=1$, $\mathbf{u}=\theta$, $\mathbf{M}=1$, $\mathbf{K}=0$, $\mathbf{s}(\theta,\dot{\theta},t)=2\beta\dot{\theta}+\sin\theta$, $\mathbf{h}_j=\mathbf{0}$, $\mathbf{f}_j(\theta,t)=\Omega A_j\sin\theta$, $\xi_j(t,\tau)=\sin((\Omega_j/\Omega)\tau+\alpha_j)$, $\tau=\Omega t$, and $\Omega=m^{-1}\sum_{j=1}^{m}\Omega_j\gg 1$.

The decision of whether to consider the linear stiffness $\Omega^2\mathbf{K}$ strong depends on whether the HFE could possibly excite linear resonances in the system. If the excitation frequencies are not well-separated from the linear natural frequencies, then the linear stiffness must be considered strong and should be put in the $\Omega^2\mathbf{K}$ term; if not, it should be represented by the $\mathbf{s}$-term. There would be no formal difficulties, for the following calculations, in letting the stiffness term be generally nonlinear and dependent of slow time, i.e. $\mathbf{Ku}=\mathbf{k}(\mathbf{u},t)$; however, since in applications a possible nonlinear part of the restoring force is typically much weaker than the linear contribution, the nonlinear part could be represented by the $\mathbf{s}$-term in Eq. (16).

The notions of 'slow' and 'fast' here refer to two distinct characteristic time scales or frequencies characterizing motions of the system: there is a time scale $t$ and a characteristic frequency $\omega$ describing motions of the system when $\xi_j=0$ for all $j$, e.g., one can take $\omega$ as the largest natural frequency of the linearized, unexcited system. It is assumed that time $t$ has been normalized such that $\omega=O(1)$. Then there is a fast time scale $\tau=\Omega t$, which describes fluctuations imposed by the external loading of characteristic HF $\Omega\gg\omega$; the time variation of such loads are given by $\xi_j$. The 'fast' loading can contain terms oscillating at many different frequencies, but some of them are high, and $\Omega$ describe their order magnitude, e.g., their average. For cases where $\Omega\gg\omega$ is not satisfied, the linear stiffness is 'strong' and should be represented by the $\Omega^2\mathbf{K}$-term as explained above.

For the general system analyzed in Ref. [12], $T=2\pi$, and the strong term $\Omega^2\mathbf{K}$ was not included. For the extension (16), the fast excitations are assumed to be generally $T$-periodic or quasi-periodic ($T\to\infty$) and to be square-integrable in $\tau$ (to justify Fourier expansion), and the strong stiffness term $\Omega^2\mathbf{K}$ extends the applicability to discrete models that arise from the mode shape expansion of continuous models of elastic structures, where the influence of resonances cannot be ignored. Many of the following results can be found also in Refs. [11,12], but is given here with special emphasis to the analysis of various stiffening effects of multi-HFE, taking also resonant influences into account.

### 3.2. An approximate set of equations governing the slow or average motions

Using the method of direct separation of motions [7] (see also Refs. [9–11]), one can separate solutions $\mathbf{u}(t)$ to Eq. (16) into slow and fast components as follows:

$$\mathbf{u}=\mathbf{u}(t,\tau)=\mathbf{z}(t)+\Omega^{-1}\boldsymbol{\varphi}(t,\tau), \tag{18}$$

where $\mathbf{z}(t)$ is the slow or average motion, and $\Omega^{-1}\boldsymbol{\varphi}$ is a rapidly oscillating overlay that has small amplitude, is $T$-periodic in the fast time $\tau=\Omega t$, and zero fast-time averages:

$$\langle\boldsymbol{\varphi}\rangle_\tau=\langle\boldsymbol{\varphi}'\rangle_\tau=\langle\boldsymbol{\varphi}''\rangle_\tau=0, \tag{19}$$

where primes denote differentiation with respect to $\tau$. Inserting into Eq. (16) and solving to first order of accuracy for $\boldsymbol{\varphi}$, one finds (see Refs. [11,12] for further details):

$$\boldsymbol{\varphi}(t,\tau)=\hat{\boldsymbol{\varphi}}(t,\tau)+O(\Omega^{-1}), \tag{20}$$

where the first approximation $\hat{\boldsymbol{\varphi}}$ for the fast motions $\boldsymbol{\varphi}$ is a particular solution of:

$$\mathbf{M}(\mathbf{z},t)\hat{\boldsymbol{\varphi}}''+\mathbf{K}\hat{\boldsymbol{\varphi}}=-\sum_{j=1}^{m}\mathbf{f}_j(\mathbf{z},t)\xi_j''(t,\tau). \tag{21}$$

Averaging Eq. (16) with Eqs. (18)–(20) inserted then gives, to first order of accuracy, a set of equations for the slow or averaged motions $\mathbf{z}$:

$$\mathbf{M}(\mathbf{z},t)\ddot{\mathbf{z}}+\Omega^2\mathbf{K}\mathbf{z}+\mathbf{s}(\mathbf{z},\dot{\mathbf{z}},t)+\mathbf{v}(\mathbf{z},\dot{\mathbf{z}},t)=\mathbf{0}, \tag{22}$$

which is similar to Eq. (16), but with the HFE terms replaced by $\mathbf{v}(\mathbf{z},\dot{\mathbf{z}},t)$, the so-called *vibrational forces* [7]:

$$\mathbf{v}(\mathbf{z},\dot{\mathbf{z}},t)=\left\langle \mathbf{s}(\mathbf{z},\dot{\mathbf{z}}+\hat{\boldsymbol{\varphi}}',t)-\mathbf{s}(\mathbf{z},\dot{\mathbf{z}},t)\right\rangle_\tau+\sum_{j=1}^{m}\left\langle \mathbf{h}_j(\mathbf{z},\dot{\mathbf{z}}+\hat{\boldsymbol{\varphi}}',t)\xi_j''(t,\tau)\right\rangle_\tau$$
$$+\sum_{j=1}^{m}\nabla\mathbf{f}_j(\mathbf{z},t)\left\langle \hat{\boldsymbol{\varphi}}\xi_j''(t,\tau)\right\rangle_\tau+\left\langle \nabla\mathbf{m}(\mathbf{z},t,\hat{\boldsymbol{\varphi}})\right\rangle_\tau, \tag{23}$$

where overdots denote differentiation with respect to $t$, and $\nabla$ denotes positional derivatives:

$$\nabla\mathbf{f}_j(\mathbf{u},t)\equiv\frac{\partial\mathbf{f}_j}{\partial\mathbf{u}}=\left[\frac{\partial\mathbf{f}_j}{\partial\mathbf{u}_{(1)}}\quad\cdots\quad\frac{\partial\mathbf{f}_j}{\partial\mathbf{u}_{(n)}}\right], \tag{24}$$

$$\nabla\mathbf{m}_{(i)}(\mathbf{u},t,\boldsymbol{\varphi})\equiv(\boldsymbol{\varphi}'')^T\nabla\mathbf{M}_{(i)}\boldsymbol{\varphi}\quad\text{where}\quad\nabla\mathbf{M}_{(i)}(\mathbf{u},t)\equiv\frac{\partial\mathbf{M}_{(i)}}{\partial\mathbf{u}}=\left[\frac{\partial\mathbf{M}_{(i)}}{\partial\mathbf{u}_{(1)}}\quad\cdots\quad\frac{\partial\mathbf{M}_{(i)}}{\partial\mathbf{u}_{(n)}}\right], \tag{25}$$

where a subscript in parenthesis denotes a vector element or matrix column. The vibrational forces $\mathbf{v}$ correspond to real physical forces having the same effect as the HFE, on the average. To an observer or measuring instrument filtering out small-amplitude HF vibrations, the response $\mathbf{u}$ from Eq. (16) is identical (within the order of approximation) to the response $\mathbf{z}$ from Eq. (22).

The initial conditions needed to solve Eq. (22) for $\mathbf{z}$ is obtained from the original initial conditions in Eq. (16), which turns into:

$$\mathbf{z}(0)=\mathbf{u}_0-\Omega^{-1}\hat{\boldsymbol{\varphi}}(0,0);\quad\dot{\mathbf{z}}(0)=\dot{\mathbf{u}}_0-\hat{\boldsymbol{\varphi}}'(0,0)-\Omega^{-1}\hat{\boldsymbol{\varphi}}(0,0), \tag{26}$$

which completes the separation of the full motions $\mathbf{u}$ into slow and fast components $\mathbf{z}$ and $\boldsymbol{\varphi}$.

Since in Eq. (22) any explicit dependence on the fast time $\tau$ has been averaged out, this equation for $\mathbf{z}$ is far easier to solve than the original equation (16) for $\mathbf{u}$. This holds not only for analytical solutions but also for numerical simulation where much larger time steps can be used, since there is no need to keep track of the rapid oscillations at frequency order of magnitude $\Omega$.

Based on the averaged system (22), a number of general results regarding HFE effects can be derived, without any need to actually solve the equations; see Ref. [12] for $\mathbf{K}=\mathbf{0}$, and Ref. [26] for a case corresponding to $\mathbf{K}\neq\mathbf{0}$. In Ref. [12] three main effects were identified and discussed: (1) *Stiffening*, which is an apparent change in the linear stiffness associated with an equilibrium, along with derived quantities such as stability and natural frequencies; (2) *biasing*, by which a system is biased towards a particular state, static or dynamic, which does not exist or is unstable in the absence of the HFE; and (3) *smoothening*, referring to a tendency for discontinuities to be effectively "smeared out" by HFE. Though these results are valid also for multi-frequency excitation ($m>1$ in Eq. (16)), no attempt was made in Ref. [12] to consider particular effects associated with this, and all specific examples were given in terms of mono-frequency harmonic excitation. Below, we focus on the effects of multi-HFE for an important subclass of Eq. (16).

### 3.3. Results for an important subclass

To illustrate the influence of multi-HFE for a simpler subclass of systems, still covering a great many applications, we assume from now a unitary mass matrix $\mathbf{M}=\mathbf{I}$ (since this could be obtained anyway by multiplying with $\mathbf{M}^{-1}$), that $\mathbf{s}$ is linear in the velocities $\dot{\mathbf{u}}$, and that the fast forces are independent of $\dot{\mathbf{u}}$. We also assume $\Omega^2\mathbf{K}=\Omega^2\boldsymbol{\omega}^2$, where $\boldsymbol{\omega}^2$ is a diagonal matrix holding the squared linear undamped natural frequencies of the system, normalized by $\Omega^2$. Note that the matrix $\Omega^2\boldsymbol{\omega}^2$ should only be given in case its components are comparable in magnitude to the squared excitation frequencies of the HFE (i.e. $|\boldsymbol{\omega}^2|=O(1)$), otherwise the corresponding forces $\mathbf{Ku}$ or accelerations $\boldsymbol{\omega}^2\mathbf{u}$ should be included in the $\mathbf{s}$-term. Then Eq. (16) becomes

$$\ddot{\mathbf{u}}+\Omega^2\boldsymbol{\omega}^2\mathbf{u}+\mathbf{s}(\mathbf{u},\dot{\mathbf{u}},t)+\sum_{j=1}^{m}\Omega\mathbf{f}_j(\mathbf{u},t)\frac{\partial^2\xi_j(t,\tau)}{\partial\tau^2}=\mathbf{0},\quad\tau=\Omega t,\quad\Omega\gg1. \tag{27}$$

The splitting of motions into slow and fast components is still given by Eq. (18) and the fast motions $\hat{\boldsymbol{\varphi}}$ given by Eqs. (20) and (21), while the averaged system (22) and (23) for the slow motions $\mathbf{z}$ becomes:

$$\ddot{\mathbf{z}} + \Omega^2\boldsymbol{\omega}^2\mathbf{z} + \mathbf{s}(\mathbf{z}, \dot{\mathbf{z}}, t) + \sum_{j=1}^{m} \nabla\mathbf{f}_j(\mathbf{z}, t)\left\langle \hat{\boldsymbol{\varphi}}\xi_j''(t,\tau)\right\rangle_\tau = \mathbf{0}. \tag{28}$$

In Eq. (28) the HF-terms of the original system (27) is replaced by the average effect of these, which takes the form of *parametrical stiffening* [11,12]. Thus the main characteristic of the subclass (27) of systems (16) is that the *smoothening* effects of HFE and certain forms of *biasing* are not covered.

Next we assume the HFE-function $\xi_j$ is time-harmonic in $t$ with high frequency $\Omega_j$ and (slowly varying or constant) phase $\alpha_j(t)$, i.e. $\xi_j(t,\tau) = \tilde{\xi}_j(t,\tau)$, where

$$\tilde{\xi}_j(t,\tau) = \sin\left(\frac{\Omega_j}{\Omega}\tau + \alpha_j(t)\right), \tag{29}$$

where the definition $\tau = \Omega t$ of fast time should be recalled, and the characteristic high frequency $\Omega$ is taken as the average excitation frequency:

$$\Omega = \frac{1}{m}\sum_{j=1}^{m} \Omega_j \gg 1. \tag{30}$$

The assumption $\xi_j(t,\tau) = \tilde{\xi}_j(t,\tau)$ is not very restrictive: Since any HFE function $\xi_j$ is already assumed to be periodic and square-integrable in $\tau$ (cf. Section 3.1), it can be Fourier-expanded into a sum of functions harmonic in $\tau$. Then Eq. (21) becomes, substituting $\tilde{\xi}_j$ for $\xi_j$ and using Eq. (29) in calculating $\xi_j''$:

$$\hat{\boldsymbol{\varphi}}'' + \boldsymbol{\omega}^2\hat{\boldsymbol{\varphi}} = \sum_{j=1}^{m} \mathbf{f}_j(\mathbf{z}, t)\,(\Omega_j/\Omega)^2\tilde{\xi}_j(t,\tau), \tag{31}$$

with particular solution:

$$\hat{\boldsymbol{\varphi}} = -\sum_{j=1}^{m} \mathbf{D}_j^{-1}\mathbf{f}_j(\mathbf{z}, t)\tilde{\xi}_j(t,\tau), \tag{32}$$

where $\mathbf{D}_j$ is the $j$th $n \times n$ diagonal *resonance matrix* corresponding to the HFE at frequency $\Omega_j$:

$$\mathbf{D}_j = \mathbf{I} - (\Omega/\Omega_j)^2\boldsymbol{\omega}^2 \tag{33}$$

where it should be recalled that $\Omega^2\boldsymbol{\omega}^2$ holds the squared natural frequencies. For excitation frequencies $\Omega_j$ much higher than the highest natural frequency, the second term in Eq. (33) is negligible so that $\mathbf{D}_j^{-1} \to \mathbf{I}$. But as an excitation frequency $\Omega_j$ approaches any of the system natural frequencies, then $|\mathbf{D}_j^{-1}| \to \infty$, and resonant oscillations of the fast motions $\hat{\boldsymbol{\varphi}}$ will occur. Since $|\hat{\boldsymbol{\varphi}}| = O(1)$ has been assumed, the following results are thus only valid when the HFE is not *sharply* resonant to the HF natural frequencies.

Inserting Eqs. (32) and (29) into Eq. (28), and using the definition (17), integration by parts, and the $T$-periodicity of $\xi_j$ and ${\xi'}_j$ one obtains

$$\ddot{\mathbf{z}} + \Omega^2\boldsymbol{\omega}^2\mathbf{z} + \mathbf{s}(\mathbf{z}, \dot{\mathbf{z}}, t) + \sum_{i,j=1}^{m} \sigma_{ij}^2(t)\nabla\mathbf{f}_i(\mathbf{z}, t)\mathbf{D}_j^{-1}\mathbf{f}_j(\mathbf{z}, t) = \mathbf{0}, \tag{34}$$

where ${\sigma_{ij}}^2$ holds the slowly varying mean-square derivatives of the HFE terms:

$$\sigma_{ij}^2(t) = \left\langle \tilde{\xi}_i'(t,\tau)\tilde{\xi}_j'(t,\tau)\right\rangle_\tau. \tag{35}$$

When $\boldsymbol{\omega}^2 = \mathbf{0}$ (i.e. the HFE frequencies are much higher than the natural frequencies), then the averaged equation (34) with Eq. (35) holds not just when $\xi_j = \tilde{\xi}_j$ as given by Eq. (29), but for any set of zero-mean $T$-periodic and square-integrable functions $\xi_i$; for that case only the mean-square derivatives count. The $\xi_j$ could even be random signals, in which case $T \to \infty$ and $\sigma^2_{\xi_j'}$ would be the covariance matrix of the HF-derivatives, and indeed results agreeing with Eqs. (34) and (35) have been obtained for multi-HFE with a randomly varying phase [18,20].

The calculation of mean-square derivatives ${\sigma_{ij}}^2$ depends on whether some of the frequencies $\Omega_j$ are close. Inserting Eq. (29) into Eq. (35) and employing Eq. (17) with $T\to\infty$ gives

$$\sigma_{ij}^2(t)=\begin{cases}\dfrac{\Omega_i\Omega_j}{2\Omega^2}\delta_{ij}, & \text{for} \quad |\Omega_i-\Omega_j|\gg 1, \quad i,j=1,\ldots,m,\\ \dfrac{1}{2}\cos\left((\Omega_i-\Omega_j)t+\alpha_i-\alpha_j\right), & \text{for} \quad |\Omega_i-\Omega_j|\leqslant O(1),\end{cases} \tag{36}$$

where $\delta_{ij}$ is the Kronecker delta, and the first case (non-close frequencies) is calculated by directly inserting Eq. (29) into Eq. (35) and using Eq. (17), while the second case (any two close frequencies) is calculated by inserting into Eq. (35) an equivalent form of Eq. (29), written in terms of the small frequency difference $\Delta\Omega_j$:

$$\tilde{\xi}_j(t,\tau)=\sin\left(\tau+\Delta\Omega_j t+\alpha_j\right), \quad \Delta\Omega_j=\Omega_j-\Omega, \quad |\Delta\Omega_j|\leqslant O(1). \tag{37}$$

As appears, for non-close frequencies the mean-square derivatives can be considered constants, while for any two close frequencies $\Omega_i$ and $\Omega_j$, the corresponding mean-square derivative ${\sigma_{ij}}^2$ is slowly oscillating in time.

### 3.4. Changes in effective properties of quasi-static equilibria

Suppose the averaged system (34) has a quasi-static equilibrium at $\mathbf{z}=\tilde{\mathbf{z}}$, i.e.:

$$\Omega^2\boldsymbol{\omega}^2\tilde{\mathbf{z}}+\mathbf{s}(\tilde{\mathbf{z}},0,t)+\sum_{i,j=1}^{m}\sigma_{ij}^2(t)\nabla\mathbf{f}_i(\tilde{\mathbf{z}},t)\mathbf{D}_j^{-1}\mathbf{f}_j(\tilde{\mathbf{z}},t)=\mathbf{0}, \tag{38}$$

at which the slowly varying derivatives w.r.t. state variables are:

$$\mathbf{K}^{\mathbf{s}}(t)=\left.\frac{\partial\mathbf{s}}{\partial\mathbf{u}}\right|_{(\mathbf{u},\dot{\mathbf{u}})=(\tilde{\mathbf{z}},\mathbf{0})}, \quad \mathbf{C}(t)=\left.\frac{\partial\mathbf{s}}{\partial\dot{\mathbf{u}}}\right|_{(\mathbf{u},\dot{\mathbf{u}})=(\tilde{\mathbf{z}},\mathbf{0})}, \tag{39}$$

$$\mathbf{K}_{ij}^{\mathbf{f}}(t)=\left.\frac{\partial(\nabla\mathbf{f}_i\mathbf{D}_j^{-1}\mathbf{f}_j)}{\partial\mathbf{u}}\right|_{\mathbf{u}=\tilde{\mathbf{z}}}=(\nabla\mathbf{f}_i\mathbf{D}_j^{-1}\nabla\mathbf{f}_j+\mathbf{f}_j^{\mathrm{T}}\otimes\nabla^2\mathbf{f}_i)|_{\mathbf{u}=\tilde{\mathbf{z}}}, \tag{40}$$

where the last term is an $m\times m$ matrix whose $k$th column is given by

$$(\mathbf{f}_j^{\mathrm{T}}\otimes\nabla^2\mathbf{f}_i)_{(k)}=\mathbf{f}_j^{\mathrm{T}}\mathbf{D}_j^{-1}(\nabla^2\mathbf{f}_i)_{(k)}, \tag{41}$$

and $(\nabla^2\mathbf{f}_i)_{(k)}$ is the Hessian matrix corresponding to $\mathbf{f}_{i(k)}$:

$$(\nabla^2\mathbf{f}_i)_{(k)}=\begin{bmatrix}\dfrac{\partial^2\mathbf{f}_{i(k)}}{\partial\mathbf{u}_{(1)}^2} & \cdots & \dfrac{\partial^2\mathbf{f}_{i(k)}}{\partial\mathbf{u}_{(1)}\partial\mathbf{u}_{(m)}}\\ \vdots & \ddots & \vdots\\ \dfrac{\partial^2\mathbf{f}_{i(k)}}{\partial\mathbf{u}_{(m)}\partial\mathbf{u}_{(1)}} & \cdots & \dfrac{\partial^2\mathbf{f}_{i(k)}}{\partial\mathbf{u}_{(m)}^2}\end{bmatrix}. \tag{42}$$

Then Eq. (34) can be Taylor-expanded at $\mathbf{z}=\tilde{\mathbf{z}}$ and rearranged into:

$$\ddot{\mathbf{z}}+\Omega^2\boldsymbol{\omega}^2\mathbf{z}+\mathbf{C}(t)\dot{\mathbf{z}}+(\mathbf{K}^{\mathbf{s}}(t)+\Delta\mathbf{K}^{\mathbf{f}}(t))(\mathbf{z}-\tilde{\mathbf{z}})+O(|\mathbf{z}-\tilde{\mathbf{z}}|^2)+O(|\dot{\mathbf{z}}|^2)=\mathbf{0}, \tag{43}$$

where

$$\Delta\mathbf{K}^{\mathbf{f}}(t)=\sum_{i,j=1}^{m}\sigma_{ij}^2(t)\mathbf{K}_{ij}^{\mathbf{f}}(t), \tag{44}$$

which governs motions near the quasi-equilibrium $\tilde{\mathbf{z}}$. Here $\Omega^2\boldsymbol{\omega}^2+\mathbf{K}^{\mathbf{s}}$ is the corresponding stiffness matrix for the system without HFE, and $\Delta\mathbf{K}^{\mathbf{f}}$ is an apparent or effective change in linear stiffness caused by the average effect of the HFE. Note that all excitation terms (those with $\mathbf{C}$, $\mathbf{K}$) in Eq. (43) are slowly varying, and purely parametric; slow *external* excitations (if present in the terms of $\mathbf{s}(\mathbf{u},\dot{\mathbf{u}},t)$ being independent of $\mathbf{u}$ and $\dot{\mathbf{u}}$) are reflected only indirectly, through slowly changing equilibrium solutions $\tilde{\mathbf{z}}(t)$ to Eq. (38).

As appears from Eq. (44) and the definition of $\mathbf{K}^{\mathbf{f}}$ in Eq. (40), for systems (27) there are two terms contributing to stiffening by HFE. The first of the two summed terms in Eq. (40) exists only if there is at least one $\mathbf{f}_j$, which is linearizable with a non-zero gradient at zero. Since this term disappears for functions that are essentially nonlinear, we term its contribution *linearly induced parametrical stiffness* (Ref. [12]). If $\langle \xi'_i\xi'_j\rangle = 0$ for $j\neq k$, as is often the case in applications, then this contribution is positive definite if all the HFE frequencies are above the highest natural frequency of oscillations, since then $\boldsymbol{\omega}^2=\mathbf{0}$, which gives $\mathbf{D}=\mathbf{I}$, so that $\nabla\mathbf{f}_i\mathbf{D}_j^{-1}\nabla\mathbf{f}_j| = |\nabla\mathbf{f}_i|\ |\mathbf{D}_j^{-1}||\nabla\mathbf{f}_j|>0$ for $i=j$. However, if some of the HFE frequencies are within the range of natural frequencies, then $|\mathbf{D}_j^{-1}|$ may be negative, and the stiffness contribution is negative, i.e. the HFE makes the system appear *less* stiff than without HFE. (Indeed this was observed experimentally in Ref. [26], where a piano string in mono-HFE showed clear drops in stiffness just below resonances.)

The second term in Eq. (40) exists only when $\mathbf{f}_j$ has both a constant and a quadratic part when Taylor-expanded near the equilibrium; we therefore term it *nonlinearly induced parametrical stiffness*, since only nonlinear functions $\mathbf{f}_j$ can contribute to it. Terms of order three and higher of the Taylor-expansion of $\mathbf{f}_j$ does not contribute to stiffness (to the level of approximation employed), since their second derivatives vanish at the equilibrium.

A change in effective stiffness implies changes in derived properties, as described next.

### 3.4.1. Change of natural frequency for oscillations near an equilibrium

The natural frequencies associated with small oscillations near an equilibrium $\tilde{\mathbf{z}}$ of the averaged system (34) are determined by the eigenvalues $\lambda=\lambda_r$, $r=1,\ \ldots,\ 2m$, which are roots of the characteristic polynomial corresponding to the linear part of Eq. (43):

$$|\lambda^2+\lambda\mathbf{C}(t)+\lambda(\Omega^2\boldsymbol{\omega}^2+\mathbf{K}^{\mathbf{s}}(t)+\Delta\mathbf{K}^{\mathbf{f}}(t))|=0, \tag{45}$$

where the time-variation of the matrices are supposed to be quasi-static. The natural frequencies (also quasi-static) are then given by $|\mathrm{Im}(\lambda_r)|$; They will generally differ from the values obtained when there is no HFE, i.e. when $\Delta\mathbf{K}^{\mathbf{f}}=\mathbf{0}$ in Eq. (45).

### 3.4.2. Shift in equilibrium position

Suppose Eq. (27) has an equilibrium at $\mathbf{u}=\tilde{\mathbf{u}}$ when there is no HFE, i.e.

$$\boldsymbol{\omega}^2\tilde{\mathbf{u}}+\mathbf{s}(\tilde{\mathbf{u}},\mathbf{0},t)=\mathbf{0}. \tag{46}$$

Then $\tilde{\mathbf{u}}$ may be different from the equilibrium(s) $\mathbf{z}=\tilde{\mathbf{z}}$ for the averaged system under HFE. The condition for an equilibrium to be unchanged under HFE is obtained by letting $\tilde{\mathbf{z}}=\tilde{\mathbf{u}}$ in Eq. (38) and inserting Eq. (46), which gives

$$\sum_{i,j=1}^{m}\sigma_{ij}^2(t)\nabla\mathbf{f}_i(\tilde{\mathbf{u}},t)\mathbf{f}_j(\tilde{\mathbf{u}},t)=\mathbf{0}\quad(\text{when }\tilde{\mathbf{u}}=\tilde{\mathbf{z}}), \tag{47}$$

from which it appears that a necessary condition for a shift in equilibrium to occur is that at least one of the functions $\mathbf{f}_j$ should be non-zero with a nonzero gradient at the equilibrium.

A small shift $\Delta\tilde{\mathbf{u}}$ in equilibrium position can be determined by Taylor-expanding Eq. (38) for $\tilde{\mathbf{z}}=\tilde{\mathbf{u}}+\Delta\tilde{\mathbf{u}}$ and solving for $\Delta\tilde{\mathbf{u}}$; this gives

$$\Delta\tilde{\mathbf{u}}=-(\Omega^2\boldsymbol{\omega}^2+\mathbf{K}^{\mathbf{s}}(t)+\Delta\mathbf{K}^{\mathbf{f}}(t))^{-1}\sum_{i,j=1}^{m}\sigma_{ij}^2(t)\nabla\mathbf{f}_i(\tilde{\mathbf{u}},t)\mathbf{D}_j^{-1}\mathbf{f}_j(\tilde{\mathbf{u}},t)+O(|\tilde{\mathbf{z}}-\tilde{\mathbf{u}}|^2). \tag{48}$$

If two or more of the HFE frequencies are close, then according to Eq. (36) $\sigma_{ij}^2$ will oscillate at the slow frequency difference, and so will the equilibrium in Eq. (48).

### 3.4.3. Change of equilibrium stability

An equilibrium $\tilde{\mathbf{z}}$ of the averaged system (34) is stable to small disturbances only if $\mathrm{Re}(\lambda_r)<0$ for all $r$, with $\lambda_r$ being the solutions of Eq. (45). Even if the HFE does not change the position of an equilibrium, i.e. $\tilde{\mathbf{z}}=\tilde{\mathbf{u}}$, the additional term $\Delta\mathbf{K}^{\mathbf{f}}$ in Eq. (45) caused by the HFE, may imply changing real parts of the eigenvalues $\lambda_r$, and thus a stable equilibrium may turn unstable or *vice versa* in the presence of HFE.

### 3.4.4. Creation of new equilibria

If solutions $\tilde{\mathbf{z}}$ to Eq. (38) exist that are not equal to or close to $\tilde{\mathbf{u}}$, we consider them as being 'new', i.e. they are created by the HFE. The stability of such equilibria can be calculated as described above.

## 4. Example II: Elastic string with multi-HFE

This example illustrates how the above general results can be used to analyze multi-HFE effects for a specific continuous, elastic system. The system is the horizontally clamped piano string in Fig. 4, whose base at the left end is vibrated horizontally at high frequency and small amplitude by an electromagnetic shaker. As appears from the figure, the string lifts in gravity in response to the HFE; this is a clear sign of the change in effective stiffness. In Ref. [26] theoretical predictions of the string lift were derived, and shown to agree with experimental results with good accuracy for a broad range of mono-HFE frequencies and amplitudes. Below we reconsider this system, but with multi-HFE. First a few experimental observations with a simple setup are presented, to illustrate qualitative features of string lift. Then follows theoretical predictions of string lift, derived from the general results of Section 3. Finally these predictions are tested experimentally, using a setup that allows accurate measurement of string lift and accurate control of the input multi-HFE.

### 4.1. Initial experimental observations with a simple setup

The initial observations were made for the string in Fig. 4, using a two-frequency harmonic HF-signal whose displacement amplitude $A$ and frequency $f=\Omega/2\pi$ are indexed 1 and 2 below, while in all cases the phase $\alpha$ was zero. The excitation frequency $f$ was controlled by software, and the excitation amplitudes $A$ were calculated as $a/(2\pi f)^2$, with $a$ being the acceleration amplitude measured by an

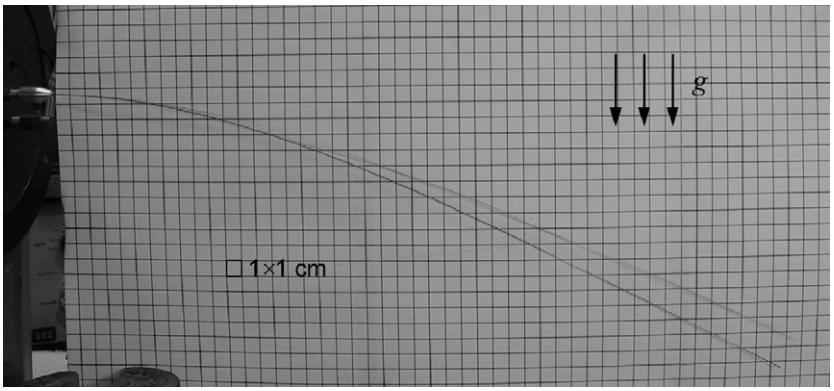


Fig. 4. Piano string ($0.5\times500\,\mathrm{mm}^2$) excited by horizontal vibrations at the base. Two images overlaid: one with gravity as the only excitation (lower string image) and one with the base vibrating horizontally at 62 Hz and 3.3 mm displacement, $500\,\mathrm{m/s}^2$ acceleration amplitude (upper image). The string tip is seen to lift about 2 cm. Camera shutter speed was 1/50 s, so the slightly blurred image of the upper string reflects positions traced during a little more than a full vibration cycle. (Adapted from Ref. [26].)

accelerometer at the shaker base. Lift of the string end was determined visually, by inspecting the string end against a non-magnetic ruler fixed immediately behind the string. The latter measurement is inaccurate, with reading errors in the range 10–25% due to the fast and slow movements of the string, and parallax, but will suffice for a first test of the theoretical predictions.

#### 4.1.1. Experiment A: Two frequency-excitation at non-close HFs

With signal 1 ($f_1 = 62\,\text{Hz}$, $a_1 = 332\,\text{m/s}^2$, $A_1 = 2.2\,\text{mm}$), the string end lifted off $u_1 \approx 6\,\text{mm}$ from the unexcited static equilibrium in gravity, this state being reached after slow oscillations of the string at its fundamental natural frequency had decayed, while small-amplitude oscillations corresponding to the HFE remained. With signal 2 ($f_2 = 138\,\text{Hz}$, $a_2 = 298\,\text{m/s}^2$, $A_2 = 0.40\,\text{mm}$), the corresponding lift of the string end was $u_2 \approx 2\,\text{mm}$. Removing either signal, the string returned to its previous, unexcited static equilibrium. Adding signals 1 and 2, the string end lifted off $u_{1+2} \approx 8.5\,\text{mm}$, with beating occurring only for the small-amplitude oscillations corresponding to the HFE. We note that $u_1 + u_2 \approx u_{1+2}$, indicating that the equilibrium shift due to stiffening could be approximately additive for each frequency component; indeed this is confirmed below. Also, the observation that no slow oscillations in the lifted equilibrium position remained, after initial transients had decayed, agrees with the general theoretical prediction (48) for multi-HFE with non-close frequencies.

#### 4.1.2. Experiment B: Two frequency-excitation at close HFs

With signal 1 equal to signal 2 ($f_1 = f_2 = 138\,\text{Hz}$, $a_1 = a_2 = 200\,\text{m/s}^2$, $A_1 = A_2 = 2.7\,\text{mm}$), the string end lifted off $u_{1+2} \approx 4.5\,\text{mm}$, which was twice as much as for signal 1 or 2 alone. However giving signal 2 a small frequency shift of 0.5 Hz ($f_2 = 138.5\,\text{Hz}$, $a_2 = 200\,\text{mm}$, $A_2 = 2.6\,\text{mm}$), the string started performing stationary slow oscillations at about 0.5 Hz, repeatingly tracing all positions between the static, unexcited equilibrium $u_{1+2} \approx 0\,\text{mm}$, and the maximum lift $u_{1+2} \approx 4.5\,\text{mm}$. These observations again support the indication of a linear additive effect, as well as the general prediction under (48) that multi-HFE with close frequencies induce effective stiffness that oscillates at the small frequency difference of the close frequencies.

#### 4.1.3. Experiment C: Band-limited HFE

Using broadband random excitation (center frequency $f = 100\,\text{Hz}$, frequency span $\Delta f = 50\,\text{Hz}$, digitally generated with frequency spacing 0.031 Hz), it was not possible to detect an average raise of the string end from its static equilibrium by the naked eye. At stronger excitation amplitudes, it started performing violent vibrations, modulated by low-frequency oscillations with seemingly random components. A similar observation was noted with narrowband excitation ($f = 62\,\text{Hz}$, $\Delta f = 3\,\text{Hz}$). These observations further support the theoretical prediction that (quasi-) stationary stiffening requires frequencies that are well separated and not sharply resonant.

### 4.2. Theoretical model predictions

#### 4.2.1. Mathematical model

The string is modeled as a viscously damped clamped–free Bernoulli–Euler beam (Fig. 5) of length $l$, mass per unit length $\rho A$, and bending stiffness $EI$. The beam vibrates in a vertical plane with configuration $u(x, t)$ in response to external forces from gravity $g$, and time-harmonic multi-HFE base excitation with HFs $\Omega_j$, small displacement amplitudes $A_j$, and phases $\alpha_j$, $j = 1, \ldots, m$. The equation of motion and boundary

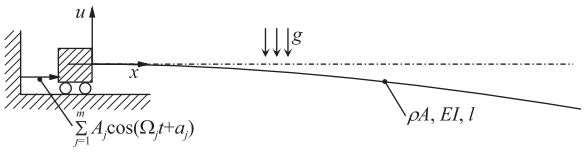


Fig. 5. Beam model of the base-excited piano string.

conditions are [26]:

$$\ddot{u} + c\dot{u} + \omega_0^2 l^4 u_{xxxx} - ((l-x)u_x)_x \sum_{j=1}^{m} \Omega_j^2 A_j \sin(\Omega_j t + \alpha_j) = -g,$$

$$\omega_0^2 = \frac{EI}{\rho A l^4}, \quad \Omega = \frac{1}{m}\sum_{j=1}^{m} \Omega_j \gg \omega_0, \quad A_j \ll l,$$

$$u(0,t) = u_x(0,t) = u_{xx}(l,t) = u_{xxx}(l,t) = 0, \tag{49}$$

where subscripts $x$ denote partial derivatives with respect to $x$, $\omega_0$ is a characteristic system frequency, and $\Omega$ a characteristic excitation frequency.

As in Ref. [26] (where $m = 1$) we use mode shape expansion for discretizing Eq. (49), i.e. let

$$u(x,t) = \mathbf{u}(t)^{\mathrm{T}} \boldsymbol{\phi}(x), \tag{50}$$

where the $n$-vector $\mathbf{u}$ holding the modal coefficients $u_i(t)$ is the new dependent variable, and the $n$-vector $\boldsymbol{\phi}$ holds the eigenfunctions $\phi_i(x)$ for a clamped–free beam [11]:

$$\phi_i(x) = \cosh\left(\frac{\lambda_i x}{l}\right) - \cos\left(\frac{\lambda_i x}{l}\right) - \frac{\cosh(\lambda_i) + \cos(\lambda_i)}{\sinh(\lambda_i) + \sin(\lambda_i)}\left(\sinh\left(\frac{\lambda_i x}{l}\right) - \sin\left(\frac{\lambda_i x}{l}\right)\right), \tag{51}$$

where $\lambda_i$ is a solution of the frequency equation $\cos(\lambda_i \cosh(\lambda_i) + 1 = 0$ (the first six approximations are $\{1.87551041,\ 4.6940911,\ 7.8547574,\ 10.995541,\ 14.137168,\ 17.278760\}$; for $i \geqslant 6$ the deviation from the asymptotic value $\lambda_i \to (2i-1)\pi/2$ is less than $10^{-7}$). The corresponding natural frequencies are

$$\omega_i = \left(\frac{\lambda_i}{l}\right)^2 \sqrt{\frac{EI}{\rho A}} = \lambda_i^2 \omega_0. \tag{52}$$

Next insert Eq. (50) into Eq. (49), multiply by $\phi_j$, integrate over the beam length, employ integration by parts, exploit the orthogonality properties of $\phi$, and obtain a set of $n$ ordinary differential equations for the modal coefficients $u$:

$$\ddot{u}_k + c\dot{u}_k + \omega_k^2 u_k + \sum_{i=1}^{n} \gamma_{ki} u_i \sum_{j=1}^{m} \Omega_j^2 A_j \sin(\Omega_j t + \alpha_j) = -\beta_k g, \quad k = 1, n, \tag{53}$$

where the modal constants $\gamma$ and $\beta$ are given by

$$\beta_k = \alpha_k^{-1} \int_0^l \phi_k \, \mathrm{d}x, \quad \gamma_{ki} = \alpha_k^{-1} \int_0^l (l-x)\phi_{kx}\phi_{ix} \, \mathrm{d}x \quad \text{where} \quad \alpha_k \equiv \int_0^l \phi_k^2 \, \mathrm{d}x. \tag{54}$$

### 4.2.2. Predictions of multi-HFE effects

In Ref. [26] the model (53) with $m = 1$ was used to predict the stiffening effect of mono-HFE for the piano string, using the method of direct separation of motions in a manner that specifically took into account the effect of resonances. This proved necessary to obtain good agreement with experimental results. Here, instead, we can use the general results of Section 3 directly, considering the influence of resonances taken into account by the matrix $\Omega^2\boldsymbol{\omega}^2$.

The discretized beam model has the general form (27) with (29), with the following correspondences of variables and parameters:

$$\mathbf{u} = \{u_1 \ldots u_n\}^{\mathrm{T}}, \quad \Omega^2\boldsymbol{\omega}^2 = \mathrm{diag}_n(\omega^2), \quad \mathbf{s}(\mathbf{u}, \dot{\mathbf{u}}, t) = c\dot{\mathbf{u}} + g\boldsymbol{\beta}, \quad \mathbf{f}_j(\mathbf{u}, t) = -\Omega A_j \boldsymbol{\gamma}\mathbf{u}, \tag{55}$$

where $\Omega^2\boldsymbol{\omega}^2$ is a diagonal matrix holding the squared natural frequencies $\omega_i^2$, the vector $\boldsymbol{\beta}$ holds $\beta_i$, and the matrix $\boldsymbol{\gamma}$ holds $\gamma_{ij}$, $i, j = 1, \ldots, n$. Then the fast component $\Omega^{-1}\hat{\boldsymbol{\varphi}}$ of the modal coefficients $\mathbf{u}$ is given by Eq. (32), while the slow or averaged component $\mathbf{z}$ is given by Eq. (34), with mean-square derivatives $\sigma_{ij}{}^2$ calculated by Eq. (36).

Focusing here on calculating string lift, which is an easily measurable characteristic of stiffness, we first use Eqs. (50) and (18) to calculate motions of the string end:

$$u(l,t) = \mathbf{u}^{\mathrm{T}}(t)\boldsymbol{\phi}(l) = \mathbf{z}(t)^{\mathrm{T}}\boldsymbol{\phi}(l) + \Omega^{-1}\boldsymbol{\varphi}(t,\tau)^{\mathrm{T}}\boldsymbol{\phi}(l), \tag{56}$$

where the slow and fast components $\mathbf{z}$ and $\Omega^{-1}\boldsymbol{\phi}$ are governed by Eqs. (34) and (32), respectively, with Eqs. (55) and (33) governed by

$$\ddot{\mathbf{z}} + \Omega^2\boldsymbol{\omega}^2\mathbf{z} + c\dot{\mathbf{z}} + \Omega^2\sum_{i,j=1}^{m}\sigma_{ij}^2 A_i A_j \boldsymbol{\gamma}\mathbf{D}_j^{-1}\boldsymbol{\gamma}\mathbf{z} = -g\boldsymbol{\beta}, \tag{57}$$

and

$$\Omega^{-1}\hat{\boldsymbol{\varphi}} = \sum_{j=1}^{m} A_j \mathbf{D}_j^{-1}\boldsymbol{\gamma}\mathbf{z}\tilde{\xi}_j, \tag{58}$$

where $\mathbf{D}_j$ is the resonance matrix (33). The stationary equilibrium $\tilde{\mathbf{z}}$ for the slow motions $\mathbf{z}$ is calculated by letting $\dot{\mathbf{z}} = \ddot{\mathbf{z}} = 0$ in Eq. (57) and solving for $\mathbf{z}$, which gives

$$\tilde{\mathbf{z}} = -g\left(\Omega^2\boldsymbol{\omega}^2 + \Omega^2\sum_{i,j=1}^{m}\sigma_{ij}^2 A_i A_j \boldsymbol{\gamma}\mathbf{D}_j^{-1}\boldsymbol{\gamma}\right)^{-1}\boldsymbol{\beta}. \tag{59}$$

In the absence of HFE (i.e. all $A_i = 0$) this gives $\tilde{\mathbf{z}} = g(\Omega\boldsymbol{\omega}^2)^{-1}$, so that the time-averaged lift of the string end becomes, using Eq. (56):

$$\begin{aligned}\Delta\tilde{u}(l) &= \left\langle \tilde{u}(l,t) - \tilde{u}_0(l,t)\right\rangle = (\tilde{\mathbf{z}}|_{A_i\neq 0} - \tilde{\mathbf{z}}|_{A_i=0})^{\mathrm{T}}\boldsymbol{\phi}(l)\\ &= g\boldsymbol{\beta}^{\mathrm{T}}\left((\Omega^2\boldsymbol{\omega}^2)^{-1} - \left(\Omega^2\boldsymbol{\omega}^2 + \Omega^2\sum_{i,j=1}^{m}\sigma_{ij}^2 A_i A_j \boldsymbol{\gamma}\mathbf{D}_j^{-1}\boldsymbol{\gamma}\right)^{-1}\right)\boldsymbol{\phi}(l).\end{aligned} \tag{60}$$

### 4.3. Case I: Non-close HFE frequencies

Inserting Eq. (36) into Eq. (60) gives, for the case of *non-close* HFE frequencies:

$$\Delta\tilde{u}(l) = g\Omega^{-2}\boldsymbol{\beta}^{\mathrm{T}}((\boldsymbol{\omega}^2)^{-1} - (\boldsymbol{\omega}^2 + \Delta\boldsymbol{\omega}^2)^{-1})\boldsymbol{\phi}(l) \quad \text{for} \quad |\Omega_i - \Omega_j| \gg 1, \tag{61}$$

where $\Omega^2\Delta\boldsymbol{\omega}^2$ holds the apparent changes in squared natural frequencies due to the HFE:

$$\Omega^2\Delta\boldsymbol{\omega}^2 = \frac{1}{2}\sum_{j=1}^{m}(\Omega_j A_j)^2\boldsymbol{\gamma}\mathbf{D}_j^{-1}\boldsymbol{\gamma}. \tag{62}$$

With $m = 1$, Eqs. (61) and (62) become identical to the expression derived under similar assumptions in Ref. [26] for mono-HFE.

If the HFE is not resonant to the system, i.e. $\mathbf{D}_j$ is not close to being singular, then $\Delta\boldsymbol{\omega}^2$ (representing HFE-generated change in stiffness) is small as compared to $\boldsymbol{\omega}^2$ (representing static structural stiffness), and it makes sense to Taylor-expand (61) to first order:

$$\Delta\tilde{u}(l) = g\boldsymbol{\beta}^{\mathrm{T}}(\Omega^2\boldsymbol{\omega}^2)^{-2}\Omega^2\Delta\boldsymbol{\omega}^2\boldsymbol{\phi}(l) \quad \text{for} \quad |\Omega_i - \Omega_j| \gg 1, \tag{63}$$

where $(\Omega^2\boldsymbol{\omega}^2)^{-2} = \mathrm{diag}(\omega_i{}^{-4})$. Thus, it appears from Eqs. (62) and (63), to the first order of approximation, the stiffening effect and corresponding string lift with non-close multi-HFE is simply linear additive. The lift resulting from a sum of non-close HFEs equals the sum of the lifts for each separate HFE. Also, when all of the HFE frequencies $\Omega_j$, $j = 1, m$, are far from the resonances $\omega_i$, $i = 1, n$, then $\mathbf{D}_j \to \mathbf{I}$ and the stiffening effect $\Omega^2\Delta\boldsymbol{\omega}^2$—and therefore the string lift $\Delta\tilde{u}(l)$—becomes simply proportional to the sum of squared HFE velocities $\sum_j(\Omega_j A_j)^2$. This agrees with the experimental observation for test $A$ in Section 4.1.1.

### 4.4. Case II: Some close HFE frequencies

Inserting Eq. (36) into Eq. (60) gives, when there are *close* HFE frequencies:

$$\Delta\tilde{u}(l) = g\Omega^{-2}\boldsymbol{\beta}^{\mathrm{T}}((\boldsymbol{\omega}^2)^{-1} - (\boldsymbol{\omega}^2 + \Delta\boldsymbol{\omega}^2 + Q(t))^{-1})\boldsymbol{\phi}(l) \quad \text{for} \quad |\Omega_i - \Omega_j| \leqslant O(1), \tag{64}$$

$$Q(t) = \frac{1}{2}\sum_{i,j=1}^{m,j\neq i} \cos((\Omega_i - \Omega_j)t + \alpha_i - \alpha_j)A_iA_j\boldsymbol{\gamma}\mathbf{D}_j^{-1}\boldsymbol{\gamma}. \tag{65}$$

Taylor-expanding again to first order gives, for a weak stiffening effect and responses that are not sharply resonant:

$$\Delta\tilde{u}(l) = g\boldsymbol{\beta}^{\mathrm{T}}(\Omega^2\boldsymbol{\omega}^2)^{-2}(\Omega^2\Delta\boldsymbol{\omega}^2 + \Omega^2 Q(t))\boldsymbol{\phi}(l) \quad \text{for} \quad |\Omega_i - \Omega_j| \gg 1, \tag{66}$$

Comparing to Eq. (63), it appears that for close frequencies, to first order of approximation, the string lifts off to the position determined as for non-close frequencies, and on top of that slow oscillations occur at an amplitude determined by the maximum of the function $Q(t)$, which depends on the particular values of the parameters in Eq. (65). This agrees qualitatively with the experimental observation for test B in Section 4.1.2. However, the experimental observation that the slow oscillations is '… tracing all positions between the static, unexcited equilibrium … and the maximum lift…' may be particular to the parameters of that experiment, since according to Eq. (66) with Eq. (65), the string end could even dip below its static equilibrium during each period of the slow oscillations.

## 5. Quantitative experimental testing

### 5.1. Experimental setup

The setup is similar to the one used in Ref. [26], including the same piano string of length 550 mm and diameter 1 mm (i.e. much stiffer than the one in Fig. 4), density 7819 kg/m and Young's modulus 195 GPa, measured lowest natural frequencies {2.4, 14.6, 40.4, 79.1, 131.0, 195.6} Hz deviating less than 1% (though 3.9% for the lowest frequency) from Bernoulli–Euler theoretical values, and linear damping ratios less than 0.3% (though 4.5% for the lowest frequency).

The string is clamped and excited horizontally by a vibration shaker at one end, as in Fig. 4. The resulting string base acceleration is measured by an accelerometer mounted at the shaker, and the time-varying string tip lift is measured by an optical tracker with an accuracy better than 0.1 mm. Measured signals are conditioned and sampled (typically at 4 kHz) by a B&K PULSE front-end unit and analyzed using B&K PULSE software. Details of the experimental setup and procedures are as described in Ref. [26], except that for the present study the newest version of B&K PULSE front-end and software were used, that this was also used for controlling the multi-frequency input to the vibration shaker, that average string lift was obtained from the zero-frequency component of the FFT of the optical tracker signal, and that root-mean-square accelerations at each input frequency was obtained from the FFT of the accelerometer signal.

### 5.2. Control parameters

A two-frequency excitation was used for the input horizontal displacement $A(t)$ at the shake base, i.e. $m = 2$ in the equations of Section 4.2, so that:

$$A(t) = A_1\sin(\Omega_1 t) + A_2\sin(\Omega_2 t); \quad \Omega_1 \neq \Omega_2. \tag{67}$$

The experimental setup allows measurements of the resulting acceleration $a(t)$ at the shaker base, as well as the root-mean-square accelerations at each input frequency $a_{i,\mathrm{rms}}$, $i = 1, 2$ so that the corresponding shaker displacements can be calculated as

$$A_i = \sqrt{2}a_{i,\mathrm{rms}}\Big/\Omega_i^2, \quad i = 1, 2. \tag{68}$$

For the presentation of results, it is convenient to express the excitation in terms of an *input acceleration* parameter $a_{\mathrm{rms}}$, which is the total rms acceleration at the shaker base, and a continuous *frequency mixing* parameter $\eta \in [0; 1]$, which is zero (unity) when all the input energy is at frequency $\Omega_1$ ($\Omega_2$) so that $(a_{1,\mathrm{rms}}/a_{\mathrm{rms}})^2 = 1-\eta$ and $(a_{2,\mathrm{rms}}/a_{\mathrm{rms}})^2 = \eta$, i.e.:

$$a_{\mathrm{rms}} = \sqrt{a_{1,\mathrm{rms}}^2 + a_{2,\mathrm{rms}}^2}, \quad \eta = (a_{2,\mathrm{rms}}/a_{\mathrm{rms}})^2. \tag{69}$$

We also define a specific input energy parameter $\bar{E} = 1/2\sum_i (\Omega_i A_i)^2$, where $\Omega_i A_i$ is the velocity amplitude at input frequency $\Omega_i$, i.e., by Eqs. (68) and (69):

$$\bar{E} = \left(\frac{a_{1,\mathrm{rms}}}{\Omega_1}\right)^2 + \left(\frac{a_{2,\mathrm{rms}}}{\Omega_2}\right)^2 = \left(\frac{1-\eta}{\Omega_1^2} + \frac{\eta}{\Omega_2^2}\right) a_{\mathrm{rms}}^2. \tag{70}$$

### 5.3. Procedures

In comparing theoretical predictions with experimental measurements, we focus on the prediction of (quasi-) *stationary average string tip lift* $\Delta\tilde{u}(l)$, since this represents the change in effective stiffness of interest here. Theoretical predictions for this are calculated using Eqs. (61) and (62) for non-close excitation frequencies, and Eqs. (64) and (65) for close frequencies. Corresponding experimental values for given excitation frequencies are obtained by (1) calibrating the optical tracker to give zero reading when the string is loaded only by gravity, i.e. without HFE, (2) imposing HFE through the shaker base, (3) waiting for stationary conditions to occur, (4) recording imposed acceleration levels at each excitation frequency from the FFT of the shaker base acceleration signal, (5) recording corresponding average string tip lift from the zero frequency component of the FFT of the optical tracker signal, (6) regularly removing the HFE to check if string tip lift reading returns to zero (recalibrating and repeating measurement if not).

Predictions for the trivial HF overlay on average tip lift can readily be obtained from the second term in Eq. (56), with $\hat{\boldsymbol{\varphi}}$ from Eq. (32) substituted for the fast motions $\boldsymbol{\varphi}$. However, this prediction is not tested separately, because the fast string motions $\boldsymbol{\varphi}$ are considered interesting only by their effect on the change in effective stiffness, i.e. only their effect "on the average" on string lift need to be correctly predicted. (Still, in Ref. [26], dealing with the mono-frequency case, excellent agreement between predicted and measured fast motions was noted.)

### 5.4. Results

Fig. 6 shows examples of measured *time series* in the form of string tip lift $\tilde{u}(l,t) - \tilde{u}_0(l,t)$ versus time at a constant input acceleration level $a_{\mathrm{rms}}$, along with measured and theoretically predicted averages (solid and dashed horizontal lines), and with parameters as given in the legend. Figs. 6(a) and (b) are for mono-frequency excitation at 61 and 110 Hz, respectively, in both cases displaying averages lifting off from zero; this reflects the stiffening effect of mono-frequency HFE as described already in Ref. [26]. The measured and predicted averages are almost indistinguishable. For Fig. 6(c) the excitations of (a) and (b) have been added into a two-frequency HFE, while keeping the same input rms-acceleration level. As appears, the string tip still lifts off to a fixed value, in-between the values of case (a) and (b), and the multi-HFE is only apparent through the overlay of two-frequency oscillations; the measured average is seen to agree with predictions (61) and (62) for the case of non-close excitation frequencies. For Fig. 6(d) the highest of the two HFE frequencies in (c) has been lowered to being only 0.5 Hz from the lowest excitation frequency. The string tip then does not settle down to a stationary average value, but lifts and drops at the slow rate of the difference frequency, still with an HF overlay corresponding to the excitation frequencies. This is in full accordance with predictions (64) and (65) for close frequencies, and the measured average still agrees with what is theoretically predicted.

Fig. 7 shows sets of *input level responses*, i.e. average string tip lifts versus (a) input acceleration $a_{\mathrm{rms}}$ and (b) input energy $\bar{E}$, for two-frequency horizontal base excitation with non-close and non-resonant frequencies $(\Omega_1, \Omega_2)/2\pi = (60, 110)$ Hz, and for five different frequency mixings. In Fig. 7(a) the set of curves from pure 60 Hz excitation ($\eta = 0$), over increasing mixings with 110 Hz excitation, to pure 110 Hz excitation ($\eta = 1$) shows decreasing lift with increased $\eta$ (reflecting that at a higher frequency the velocity amplitude and therefore

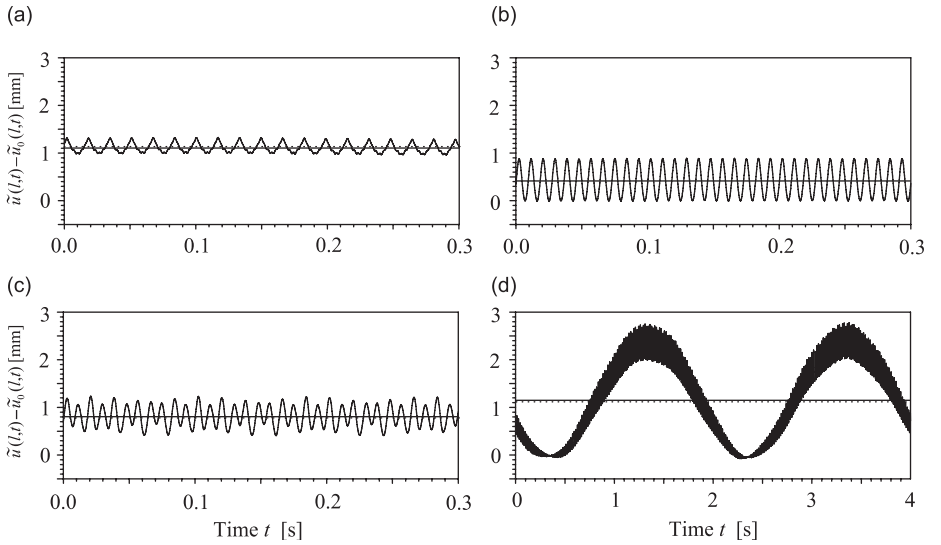


Fig. 6. Measured string tip lift $\tilde{u}(l,t)-\tilde{u}_0(l,t)$ versus time for the $1\times550\,\mathrm{mm}^2$ horizontal string at input base acceleration $a_{\mathrm{rms}}=300/\sqrt{2}\,\mathrm{m/s}^2$ and (a) mono-frequency excitation ($\eta=0$) at $\Omega_1/2\pi=61\,\mathrm{Hz}$; (b) mono-frequency excitation ($\eta=1$) at $\Omega_2/2\pi=110\,\mathrm{Hz}$; (c) two-frequency excitation ($\eta=0.5$) at non-close frequencies $(\Omega_1,\ \Omega_2)/2\pi=(61,\ 110)\,\mathrm{Hz}$; (d) two-frequency excitation ($\eta=0.5$) at close frequencies $(\Omega_1,\ \Omega_2)/2\pi=(61,\ 61.5)\,\mathrm{Hz}$. Curves: experimentally measured time series (stationary conditions); Solid horizontal line: times series average; Dashed horizontal line: theoretically predicted average $\Delta\tilde{u}(l)$ by Eqs. (61) and (62). System parameters: $L=0.55\,\mathrm{m}$, $E=195\times10^9\,\mathrm{Pa}$, $g=9.82\,\mathrm{m/s}^2$, $\rho A=6.1410\times10^{-3}\,\mathrm{kg/m}$, $EI=9.5720\times10^{-3}\,\mathrm{N\,m}^2$, $\rho Ac=8\times10^{-3}\,\mathrm{kg/m/s}$, $n=6$ modes.

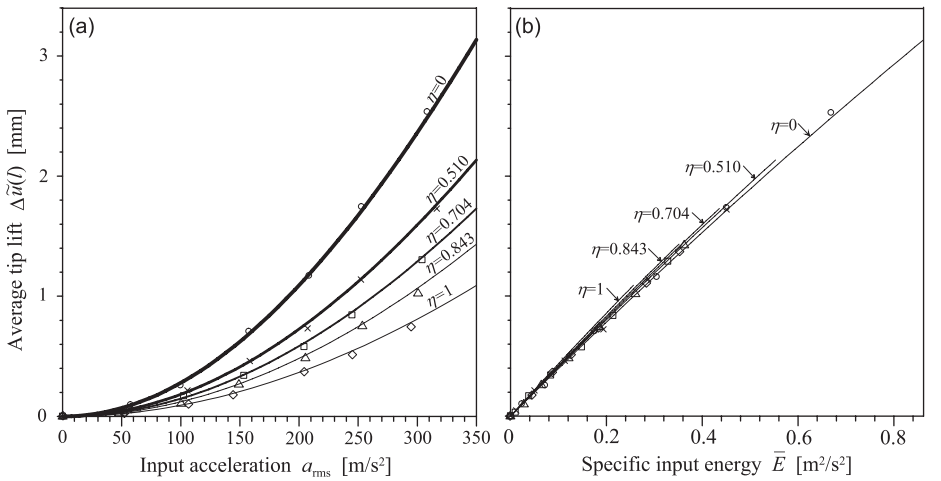


Fig. 7. Average string tip lift $\Delta\tilde{u}(l)$ for the $1\times550\,\mathrm{mm}^2$ horizontal string with two-frequency horizontal base excitation $(\Omega_1,\ \Omega_2)/2\pi=(60,\ 110)\,\mathrm{Hz}$, as a function of (a) input acceleration $a_{\mathrm{rms}}$ and (b) input energy $\bar{E}$, for five different frequency mixings $\eta$. Lines: theoretical predictions by Eqs. (61) and (62); marker symbols: experimentally measured. System parameters as for Fig. 6.

energy input must decrease to keep the acceleration level fixed), and also a nearly quadratic increase of string tip lift with acceleration level (reflecting the quadratic term in Eq. (62)). It also appears that the experimentally measured values (symbol markers) are in good agreement with the theoretical predictions. Fig. 7(b) shows the same theoretical and experimental data as Fig. 7(a), but plotted instead with the specific input energy $\bar{E}$ as the input level variable. As appears, all the data cluster around the same almost straight line. This reflects the prediction stated under Eq. (63), that for non-close and non-resonant HFE, stiffening (and thus string lift) grows simply with the sum of squared HFE velocities $\sum_i(\Omega_i A_i)^2=2\bar{E}$, while the particular mixing of excitation frequencies is less relevant.

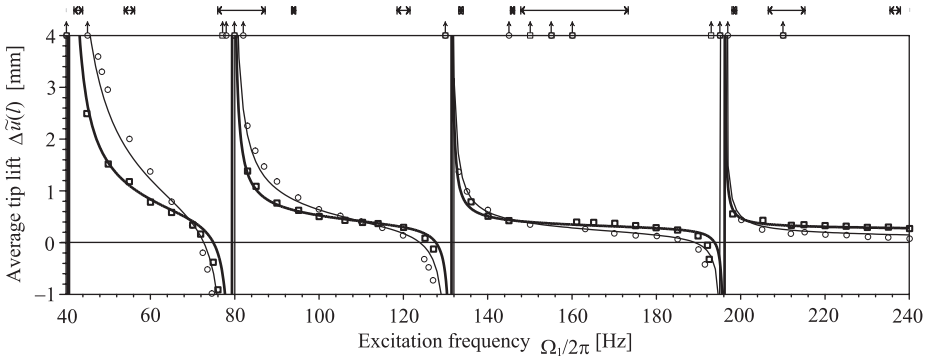


Fig. 8. Average string tip lift $\Delta\tilde{u}(l)$ for the $1\times550\,\mathrm{mm}^2$ horizontal string with constant horizontal input acceleration $a_{\mathrm{rms}}=300/\sqrt{2}\,\mathrm{m/s}^2$, constant second excitation frequency $\Omega_2/2\pi=110\,\mathrm{Hz}$, and quasi-statically varied first excitation frequency $\Omega_1/2\pi_1\in[0;\,240]$ Hz. Lines: theoretical predictions by Eqs. (61) and (62); thick line: $\eta=0.5$ (i.e. two-frequency excitation with $a_{1,\mathrm{rms}}=a_{2,\mathrm{rms}}=150\,\mathrm{m/s}^2$); thin line: $\eta=0$ (i.e. mono-frequency excitation with $a_{1,\mathrm{rms}}=300/\sqrt{2}\,\mathrm{m/s}^2$, $a_{2,\mathrm{rms}}=0$); marker symbols: experimentally measured (with up-pointing arrows indicating large resonant response). Horizontal arrow lines above the graph span theoretically predicted ranges of parametric resonance. System parameters as for Fig. 6.

Fig. 8 shows two *frequency responses*, i.e. average string lift versus input excitation frequency $\Omega_1$. The curve in thin line is for mono-frequency HFE ($a_{2,\mathrm{rms}}=0$), while the one in thick line is for two-frequency excitation with $\eta=0.5$. In the later case, as $\Omega_2$ is kept constant at 110 Hz, $\Omega_1$ is varied (quasi-statically) over the range 0–240 Hz, keeping the total acceleration level at $a_{\mathrm{rms}}=300/\sqrt{2}\,\mathrm{m/s}^2$. The swept range includes the natural frequencies at 40, 79, 131, and 196 Hz, and thus tests the capability of the theoretical predictions to include effects of resonance on stiffening. It should be emphasized that the figure does *not* show the amplitude of string vibrations, as would a usual frequency response, but shows the *average lift* of the string tip (undergoing HF oscillations) under stationary conditions. As appears, for both the mono- and the two-frequency case, the string generally lifts off from zero (i.e., is stiffened) by the HFE, most pronounced just above the natural frequencies. However, at excitation frequencies just below the natural frequencies, the string tip *drops down* under zero, reflecting a *negative stiffening* effect at these frequencies, where the string appears more flexible with than without HFE. The main effect of two-frequency excitation, as compared to the mono-frequency case, appears to be a *flattening* of the non-resonant parts of the response curve. But this just reflects the fact that in the two-frequency case some of the input energy goes to $\Omega_2$ leaving less for the sweep frequency $\Omega_1$; ultimately, as $\eta\to1$ and all energy goes to $\Omega_2$, the frequency response will be all flat, taking on the constant value of the string lift corresponding to the HFE at $\Omega_2$. As also appears, the experimentally measured values (symbol markers) for both the mono- and the two-frequency case are in good agreement with the theoretical predictions, even close to natural frequencies. At some excitation frequencies the string exhibits strongly resonant behavior (up-pointing arrows in the Fig. 8). These frequencies are either very close to natural frequencies of the string (curve spikes in the Fig. 8) or within or close to theoretically predicted frequency ranges of *parametric* resonance (horizontal arrow lines above the Fig. 8); see Ref. [26] for more details on parametric resonances for this string system.

The results presented in this section demonstrates how the effective stiffness for a flexible structure is affected by mono- and two-frequency HFE, illustrates how to employ the general theoretical results of Section 3 for predicting effective stiffening, and proves good agreement between theory and experimental measurements for a rather wide range of excitation conditions.

## 6. Conclusions

- Strong parametrical HFE at multiple frequencies has a stiffening effect on mechanical systems, which is similar to that of mono-frequency excitation, provided the excitation frequencies are well separated.
- For non-close and non-resonant excitation frequencies, the change in effective static stiffness is proportional to the sum of squared excitation velocities, i.e. to the input energy level.

- With two or more close excitation frequencies, there is an additional contribution of slowly oscillating stiffness, having magnitude order similar to the change in static stiffness, and frequencies equal to the differences in non-close frequencies.
- With close excitation frequencies, strong parametric resonance can occur at conditions that might not appear obvious, that is when the difference in any two excitation frequencies comes near $2\tilde{\omega}/k$, where $k$ is an integer (with $k = 1$ corresponding to primary parametric resonance), and $\tilde{\omega}$ is an effective natural frequency of the system, which due to the HFE is shifted away from the natural frequency $\omega$ without HFE.
- Strong multi-frequency HFE can stabilize unstable quasi-static equilibria. Generally this holds only if the frequencies are well separated, i.e. with differences much larger than the lowest natural frequencies of the system. With two or more close high frequencies, the effect of HFE may be stabilizing or destabilizing, depending on particular parameter values. Thus continuous broadband and random excitation does not have a uniquely stabilizing effect paralleling that of mono-frequency HFE, or multi-frequency HFE with non-close frequencies.
- The above conclusions were derived for a class of generally nonlinear systems subjected to strong multi-frequency HFE of an arbitrary period, and illustrated for a simple pendulum system with a vibrating support, and for a parametrically excited horizontal flexible beam in gravity. For the latter example, comparison of theoretical predictions with experimental measurement for a wide range of excitation conditions showed good agreement on all aspects of concern.
- The general results may be used to investigate or utilize general effects, or as a shortcut for calculating effective properties for specific systems, or for calculating averaged equations of motion that may be much faster to simulate numerically.

## References


[1] J.J. Thomsen, Computing effective properties of nonlinear structures exposed to strong high-frequency loading at multiple frequencies, in: C.A. Mota Soares et al. (Eds.), *ECCM 2006 CD-ROM Proceedings*, *III European Conference on Computational Mechanics*, Lisbon, Portugal, 5–9 June 2006, Springer, Lisbon, Portugal, 2006, p. 20.

[2] A. Stephenson, On a new type of dynamic stability, *Memoirs and Proceedings of the Manchester Literary and Philosophical Society* 52 (1908) 1–10.

[3] P.L. Kapitza, Dynamic stability of a pendulum with an oscillating point of suspension, *Zurnal Eksperimental'noj i Teoreticeskoj Fiziki* 21 (1951) 588–597 (in Russian).

[4] V.N. Chelomei, On the possibility of increasing the stability of elastic systems by using vibration, *Doklady Akademii Nauk SSSR* 110 (1956) 345–347 (in Russian).

[5] I.I. Blekhman, Method of direct motion separation in problems of vibration acting on nonlinear mechanical systems, *Mechanics of Solids* 11 (1976) 7–19.

[6] V.N. Chelomei, Mechanical paradoxes caused by vibrations, *Soviet Physics Doklady* 28 (1983) 387–390.

[7] I.I. Blekhman, *Vibrational Mechanics-Nonlinear Dynamic Effects, General Approach, Applications*, World Scientific, Singapore, 2000.

[8] J.S. Jensen, Non-trivial Effects of Fast Harmonic Excitation, PhD Thesis, Department of Solid Mechanics, Technical University of Denmark, DCAMM Report, S83, 1999.

[9] I.I. Blekhman, Selected topics in vibrational mechanics, in: I.I. Blekhman, A. Guran (Eds.), *Series A on Stability, Vibration, and Control of Systems*, World Scientific, Singapore, 2004.

[10] A. Fidlin, *Nonlinear Oscillations in Mechanical Engineering*, Springer, Berlin, Heidelberg, 2005.

[11] J.J. Thomsen, *Vibrations and Stability: Advanced Theory, Analysis, and Tools*, Springer, Berlin, Heidelberg, 2003.

[12] J.J. Thomsen, Some general effects of strong high-frequency excitation: stiffening, biasing, and smoothening, *Journal of Sound and Vibration* 253 (2002) 807–831.

[13] J.J. Thomsen, Slow high-frequency effects in mechanics: problems, solutions, potentials, *International Journal of Bifurcation and Chaos* 15 (2005) 2799–2818.

[14] A.H. Nayfeh, D.T. Mook, *Nonlinear Oscillations*, Wiley, New York, 1979.

[15] A.H. Nayfeh, The response of non-linear single-degree-of-freedom systems to multifrequency excitations, *Journal of Sound and Vibration* 102 (1985) 403–414.

[16] S.A. Nayfeh, A.H. Nayfeh, The response of nonlinear systems to modulated high-frequency input, *Nonlinear Dynamics* 7 (1995) 301–315.

[17] S.V. Chelomei, Dynamic stability upon high-frequency parametric excitation, *Soviet Physics Doklady* 26 (1981) 390–392.

[18] J.L. Bogdanoff, S.J. Citron, Experiments with an inverted pendulum subject to random parametric excitation, *Journal of the Acoustical Society of America* 38 (1965) 447–452.

[19] G.W. Hemp, P.R. Sethna, On dynamical systems with high frequency parametric excitation, *International Journal of Non-Linear Mechanics* 19 (1968) 351–365.

[20] A.S. Kovaleva, Stabilization of a quasi-conservative system subjected to high frequency excitation, *Journal of Applied Mathematics and Mechanics* 65 (2001) 895–905.
[21] J.S. Jensen, Buckling of an elastic beam with added high-frequency excitation, *International Journal of Non-Linear Mechanics* 35 (2000) 217–227.
[22] D.M. Tcherniak, The influence of fast excitation on a continuous system, *Journal of Sound and Vibration* 227 (1999) 343–360.
[23] J.S. Jensen, D.M. Tcherniak, J.J. Thomsen, Stiffening effects of high-frequency excitation: experiments for an axially loaded beam, *ASME Journal of Applied Mechanics* 67 (2000) 397–402.
[24] M.H. Hansen, Effect of high-frequency excitation on natural frequencies of spinning disks, *Journal of Sound and Vibration* 234 (2000) 577–589.
[25] J.J. Thomsen, D.M. Tcherniak, Chelomei's pendulum explained, *Proceedings of the Royal Society of London A* 457 (2001) 1889–1913.
[26] J.J. Thomsen, Theories and experiments on the stiffening effect of high-frequency excitation for continuous elastic systems, *Journal of Sound and Vibration* 260 (2003) 117–139.
[27] D. Tcherniak, J.J. Thomsen, Slow effects of fast harmonic excitation for elastic structures, *Nonlinear Dynamics* 17 (1998) 227–246.
[28] I.I. Blekhman, P.S. Landa, Conjugate resonances and bifurcations in nonlinear systems under biharmonical excitation, *International Journal of Non-Linear Mechanics* 39 (2004) 421–426.